

# Quantifying the Relationship Between Genetic Diversity and Population Size Suggests Natural Selection Cannot Explain Lewontin's Paradox

Vince Buffalo<sup>1\*</sup>

\*For correspondence:  
vsbuffalo@gmail.com (VB)

<sup>1</sup> Institute of Ecology and Evolution, University of Oregon, United States

## Abstract

Neutral theory predicts that genetic diversity increases with population size, yet observed levels of diversity across metazoans vary only two orders of magnitude while population sizes vary over several. This unexpectedly narrow range of diversity is known as Lewontin's Paradox of Variation (1974). While some have suggested selection constrains diversity, tests of this hypothesis seem to fall short. Here, I revisit Lewontin's Paradox to assess whether current models of linked selection are capable of reducing diversity to this extent. To quantify the discrepancy between pairwise diversity and census population sizes across species, I combine previously-published estimates of pairwise diversity from 172 metazoan taxa with newly derived estimates of census sizes. Using phylogenetic comparative methods, I show this relationship is significant accounting for phylogeny, but with high phylogenetic signal and evidence that some lineages experience shifts in the evolutionary rate of diversity deep in the past. Additionally, I find a negative relationship between recombination map length and census size, suggesting abundant species have less recombination and experience greater reductions in diversity due to linked selection. However, I show that even assuming strong and abundant selection, models of linked selection are unlikely to explain the observed relationship between diversity and census sizes across species.

## Introduction

A longstanding mystery in evolutionary genetics is that the observed levels of genetic variation across sexual species span an unexpectedly narrow range. Under neutral theory, the average number of nucleotide differences between sequences (pairwise diversity,  $\pi$ ) is determined by the balance of new mutations and their loss by genetic drift (???). In particular, expected pairwise diversity at neutral sites in a panmictic population of  $N_c$  diploids is  $\pi \approx 4N_c\mu$ , where  $\mu$  is the per basepair per generation mutation rate. Given that metazoan germline mutation rates only differ 10-fold ( $10^{-8}$ – $10^{-9}$ , ??), and census sizes vary over several orders of magnitude, under neutral theory one would expect that pairwise diversity also vary over several orders of magnitude. However, early allozyme surveys revealed that diversity levels across a wide range of species varied just an order of magnitude (?, p. 208); this is known as Lewontin's "Paradox of Variation". With modern sequencing-based estimates of  $\pi$  across taxa ranging over only three orders of magnitude (0.01–10%, ?), Lewontin's paradox remains unresolved through the genomics era.

39 Early on, explanations for Lewontin's Paradox have been framed in terms of the neutralist-  
 40 selectionist controversy (????). The neutralist view is that beneficial alleles are sufficiently rare  
 41 and deleterious alleles are removed sufficiently quickly, that levels of genetic diversity are shaped  
 42 predominantly by genetic drift and mutation (?). Specifically, *non-selective* processes decouple the  
 43 effective population size implied by observed levels of diversity  $\hat{\pi}$ ,  $\tilde{N}_e = \hat{\pi}/4\mu$ , from the census size,  
 44  $N_c$ . By contrast, the selectionist view is that direct selection and the indirect effects of selection  
 45 on linked neutral diversity suppress diversity levels across taxa, specifically because the impact  
 46 of linked selection is greater in large populations. Undoubtedly, these opposing views represent  
 47 a false dichotomy, as population genomic studies have uncovered evidence for the substantial  
 48 impact of both demographic history (e.g. ??) and linked selection on genome-wide diversity (e.g.  
 49 ???).

## 50 Possible Resolutions of Lewontin's Paradox

51 A resolution of Lewontin's Paradox would involve a mechanistic description and quantification of  
 52 the evolutionary processes that prevent diversity from scaling with census sizes across species.  
 53 This would necessarily connect to the broader literature on the empirical relationship between di-  
 54 versity and population size (????), and the ecological and life history correlates of genetic diversity  
 55 (???). Three categories of processes stand out as potentially capable of decoupling census sizes  
 56 from diversity: non-equilibrium demography, variance and skew in reproductive success, and se-  
 57 lective processes.

58 It has long been appreciated that effective population sizes are typically less than census popula-  
 59 tion sizes, tracing back to early debates between R.A. Fisher and Sewall Wright (?). Possible causes  
 60 of this divergence between effective and census population sizes include demographic history (e.g.  
 61 population bottlenecks), extinction and recolonization dynamics, or the breeding structure of popu-  
 62 lations (e.g. the variance in reproductive success and population substructure). Early explanations  
 63 for Lewontin's Paradox suggested bottlenecks during the last glacial maximum severely reduced  
 64 population sizes (???), and emphasized that large populations recover to equilibrium diversity lev-  
 65 els more slowly (?, ? p. 203-204). Another explanation is that cosmopolitan species repeatedly  
 66 endure extinction and recolonization events, which reduces effective population size (?).

67 While intermittent demographic events like bottlenecks and recent expansions have long-term  
 68 impacts on diversity (since mutation-drift equilibrium is reached on the order of size of the popu-  
 69 lation), characteristics of the breeding structure such as high variance ( $V_w$ ) or skew in reproductive  
 70 success continuously suppress diversity below the levels predicted by the census size (?). For ex-  
 71 ample, in many marine animals, females are highly fecund, and dispersing larvae face extremely  
 72 low survivorship, leading to high variance in reproductive success (????). Such "sweepstakes" re-  
 73 productive systems can lead to remarkably small ratios of effective to census population size (e.g.  
 74  $N_e/N_c$  can range from  $10^{-6}$ – $10^{-2}$ ), since  $N_e/N \approx 1/V_w$  (????), and require multiple-merger coalescent pro-  
 75 cesses to describe their genealogies (?). Overall, these reproductive systems diminish the diversity  
 76 in some species, but seem unlikely to explain Lewontin's Paradox broadly across metazoans.

77 Alternatively, selective processes, and in particular the indirect effects of selection on linked  
 78 neutral variation, could potentially explain the observed narrow range of diversity. The earliest  
 79 mathematical model of hitchhiking was proffered as an explanation of Lewontin's Paradox (?). Since,  
 80 linked selection has been shown to impact diversity levels in a variety of species, as evidenced by  
 81 the correlation between recombination and diversity (????). Theoretic work to explain this pat-  
 82 tern has considered the impact of a steady influx of beneficial mutations (recurrent hitchhiking;  
 83 ??), and purifying selection against deleterious mutations (background selection, BGS; ???). In-  
 84 deed, empirical work indicates background selection diminishes diversity around genic regions in  
 85 a variety of species (???), and now efforts have shifted towards teasing apart the effects of positive  
 86 and negative selection on genomic diversity (?).

87 A class of models that are of particular interest in the context of Lewontin's Paradox are recur-  
 88 rent hitchhiking models that decouple diversity from the census population size. These models pre-

dict diversity levels when strongly selected beneficial mutations regularly enter and sweep through the population, trapping lineages and forcing them to coalesce (??). In general, decoupling occurs under these hitchhiking models when the rate of coalescence due to selection is much greater than the rate of neutral coalescence (e.g. ?, equation 22). In contrast, under other linked selection models, the resulting effective population size is proportional to population size; these models cannot decouple diversity, all else equal. For example, models of background selection and polygenic fitness variation predict diversity is proportional to population size, mediated by the total recombination map length and the deleterious mutation rate or fitness variation (??????).

## Recent Approaches Towards Resolving Lewontin's Paradox

Recently, ? used population genomic data to estimate the reduction in diversity due to background selection and hitchhiking across 40 species, and showed that the impact of selection increases with two proxies of census population size, species range and with body size. Based on this evidence, they argued that selection could explain Lewontin's Paradox; however, in a re-analysis, ? demonstrated that the observed magnitude of these reductions is insufficient to explain the orders-of-magnitude shortfall between observed and expected levels of diversity across species. Other recent work has found that life history characteristics related to parental investment, such as propagule size, are good predictors diversity in animals (??). Nevertheless, while these diversity correlates are important clues, they do not propose a mechanism by which these traits act to constrain diversity within a few orders of magnitude.

Here, I revisit Lewontin's Paradox by integrating several data sets in order to compare the observed reductions between diversity and census size with the predicted relationship under different selection models. Prior surveys of genetic diversity either lacked census population size estimates, used allozyme-based measures of heterozygosity, or included fewer species. To address these shortcomings, I first estimate census sizes by combining predictions of population density based on body size with ranges estimated from geographic occurrence data. Using these estimates, I quantify the relationship between census size and previously-published genomic diversity estimates across 172 metazoan taxa within nine phyla, thus characterizing the relationship between  $\pi$  and  $N_c$  that underlies Lewontin's Paradox.

Past work looking at the relationship between  $\pi$  and  $N_c$  has been unable to fully account for phylogenetic non-independence across taxa (?). To address this, I use phylogenetic comparative methods (PCMs) with a synthetic time-calibrated phylogeny to account for shared phylogenetic history. Moreover, it is disputed whether considering phylogenetic non-independence is necessary in population genetics, given that coalescent times within species are much less than divergence times (??). Using PCMs, I address this by estimating the degree of phylogenetic signal in the diversity census size relationship, and investigating how these traits evolve along the phylogeny.

Finally, I explore whether the predicted reductions of diversity under background selection and recurrent hitchhiking are sufficiently strong to resolve Lewontin's Paradox. I do so using selection parameters from *Drosophila melanogaster*, a species known to be strongly affected by linked selection. Given the effects of linked selection are mediated by recombination map length, I also investigate how recombination map lengths vary with census population size using data from a previously-published survey (?). I find map lengths are typically shorter in large-census-size species, increasing the effects of linked selection in these species, which could further decouple diversity from census size. Still, I find the combined impact of these modes of linked selection fall short in explaining Lewontin's Paradox, and discuss future avenues through which the Paradox of Variation could be fully resolved.

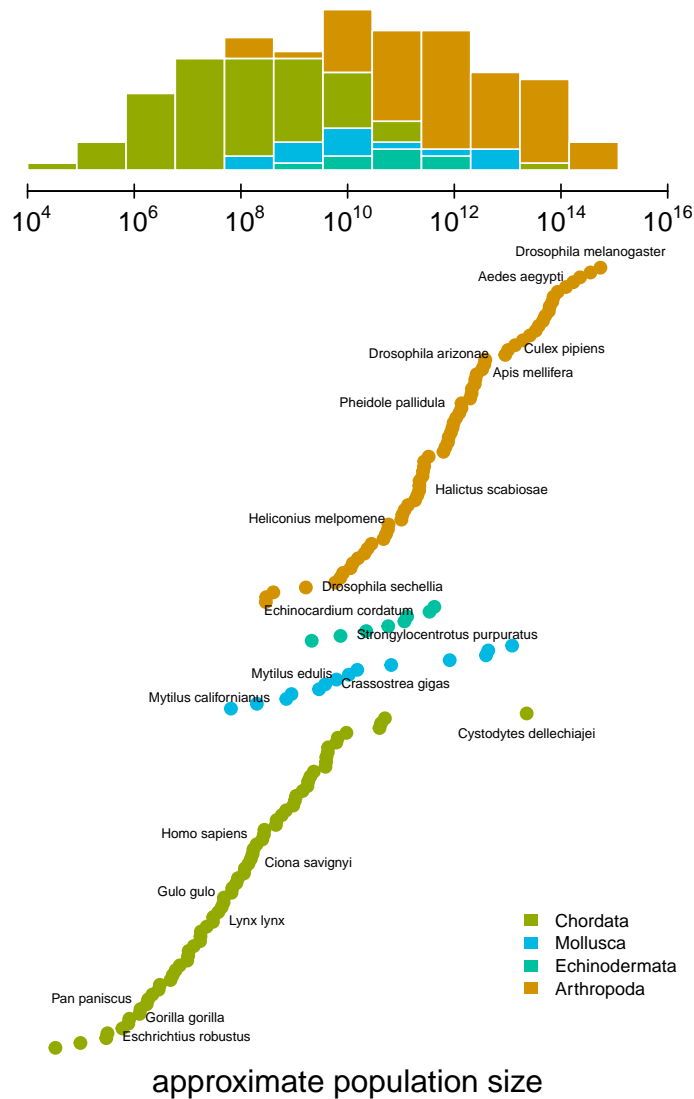


**Figure 1.** The distribution of approximate census population sizes estimated by this study. Some phyla containing few species were excluded for clarity.

**Figure 1–Figure supplement 1.** The relationship between body mass and population density found by ?, which is used to predict population densities.

**Figure 1–Figure supplement 2.** The fraction of total species per class on earth included in this study's sample, per class.

**Figure 1–Figure supplement 3.** Comparison of this paper's range estimates procedure against the IUCN Red List's range estimates.

**Figure 1–Figure supplement 4.** Validation of this paper's range estimates against the categorical labels of ?.

**Figure 1–Figure supplement 5.** The relationship between body length (meters) and body mass (grams) in the ? data set.

**Figure 1–source data 1.** The population size estimates for 172 metazoan taxa.

## Results

### Estimates of Census Population Size

An impediment in resolving Lewontin's Paradox is characterizing the relationship between diversity and census population sizes. This is difficult because census population sizes are unavailable for many taxa, especially for extremely abundant, cosmopolitan species that define the upper limit of ranges. Previous work has surveyed the literature for census size estimates (??), or used range, body size, or qualitative categories as proxies for census size (??). To quantify the relationship between genomic estimates of diversity and census population sizes, I first approximate census population sizes for 172 metazoan taxa (??). I estimate population densities based on an empirical linear relationship between body sizes and density that holds across metazoans (see ??-??; ??). Then, from geographic occurrence data, I estimate range sizes. Finally, I estimate population size as the product of these predicted densities and range estimates (see Methods and Materials: ??). Note that the relationship between population density and body size is driven by energy budgets, and thus reflects macroecological equilibria (?). Consequently, population sizes are underestimated for taxa like humans and their domesticated species, and overestimated for species with anthropogenically reduced densities or fragmented ranges. For example, the population size of *Lynx lynx* is likely around 50,000 (?) which is around two orders of magnitude smaller than my estimate. Additionally, the range size estimates do not consider whether an area has unsuitable habitat, and thus may be overestimated for species with particular niches or patchy habitats. While my approach produces approximate and sometimes crude estimates, it has the advantage that it can be efficiently calculated for numerous taxa, which is sufficient to estimate the magnitude of Lewontin's Paradox (see ?? for more on validation based on biomass and other approaches).

### Characterizing the Diversity-Census-size Relationship

To determine which ecological or evolutionary processes could decouple diversity from census population size, we first need to quantify this relationship across a wide variety of taxa. Previous work has found there is a significant relationship between heterozygosity and the logarithm of population size or range size, but these studies relied on heterozygosity measured from allozyme data (???). I confirm these findings using pairwise diversity estimates from genomic sequence data and the estimated census sizes (??). The pairwise diversity estimates are from three sources: ?, ?, and ?, and are predominantly from either synonymous or non-coding DNA (see Methods and Materials: ??). Overall, an ordinary least squares (OLS) relationship on a log-log scale fits the data well (??, gray dashed line). The OLS slope estimate is significant and implies a 13% percent increase in differences per basepair for every order of magnitude census size grows (95% confidence interval [12%, 14%], adjusted  $R^2 = 0.26$ ; see also the OLS fit per-phylo, ??-??).

Notably, this relationship has few outliers and is relatively homoscedastic. This is in part because of the log-log scale, in contrast to previous work (??); see ??-?? for a version on a log-linear scale. However, it is noteworthy that few taxa have diversity estimates below  $10^{-3.5}$  differences per basepair. Those that do, lynx (*Lynx lynx*), wolverine (*Gulo gulo*), and Massasauga rattlesnake (*Sistrurus catenatus*) face habitat loss and declining population sizes. These three species are all in the IUCN Red List, but are listed as least concern (though their presence in the Red List indicates they are of conservation interest). In Appendix ??, ??, I explore the relationships between IUCN Red List status, diversity, and population size.

### Phylogenetic Non-Independence and the Population Size Diversity Relationship

One limitation of using ordinary least squares is that shared phylogenetic history can create correlation structure in the residuals, which violates an assumption of the regression model and can lead to bias (??). To address this shortcoming, I fit the diversity-census-size relationship using a phylogenetic mixed-effects model, investigated whether there is a signal of phylogenetic non-independence, estimated the continuous trait values on the phylogeny, and explored how



diversity and population size evolve. Prior population genetic comparative studies have lacked time-calibrated phylogenies and assumed unit branch lengths (?), a shortcoming that has drawn criticism (?). I use a synthetic time-calibrated phylogeny created from the DateLife project (?) to account for shared phylogenetic history (see Methods and Materials: ??).

Using a phylogenetic mixed-effects model (???) implemented in Stan (??), I estimated the linear relationship between diversity and population size (on a log-log scale) accounting for phylogeny, for the 166 taxa without missing data and present in the synthetic chronogram. This phylogenetic mixed-effects model can account for correlated residuals among more closely related species when estimating the relationship between  $N_c$  and  $\pi$ , but does not assume there is phylogenetic signal in either of these variables. Since the phylogenetic mixed-effects model simultaneously estimates the degree of phylogenetic structure in the residuals while fitting the relationship between  $N_c$  and  $\pi$ , this model's estimates would match those found by ordinary least squares if the residuals were distributed independently. Overall, this approach is conservative, making no assumptions about the source of the phylogenetic signal while accounting for violations of the regression model due to dependence among the residuals (see ? for a discussion of this).

As with the linear regression, I find this relationship is positive and significant (95% credible interval 0.03, 0.11), though somewhat attenuated compared to the OLS estimates (??B). Since the population size estimates are based on range and body mass, they are essentially a composite trait; fitting phylogenetic mixed-effects models separately on body mass and range indicates these have significant negative and positive effects, respectively (??-??; see also ??-?? for the relationship between diversity and the range categories of ?).

Since the phylogenetic mixed-effects model simultaneously estimates the variance of the phylogenetic effect ( $\sigma_p^2$ ) and the residual variance ( $\sigma_r^2$ ), these can be used to estimate the phylogenetic signal,  $\lambda = \sigma_p^2 / (\sigma_p^2 + \sigma_r^2)$  (??; see ? for a comparison to Pagel's  $\lambda$ ). If the residuals were free of correlations due to shared phylogenetic history, then  $\lambda = 0$  and all the variance could be explained by evolution on the tips; this is analogous to Lynch's conjecture that coalescent times should be free of phylogenetic signal (?). In the relationship between population size and diversity, the posterior mean of  $\lambda = 0.67$  (90% credible interval [0.58, 0.75]) indicates a majority of the variance perhaps might be due to shared phylogenetic history (??B).

This high degree of phylogenetic signal suggests ?'s (1991) concern that the  $\pi$ - $N_c$  relationship was driven by chordate-arthropod differences may be valid. A visual inspection of the estimated ancestral continuous values for diversity and population size on the phylogeny indicates the high phylogenetic signal seems to be driven in part by chordates having low diversity and small population sizes compared to non-chordates (??A). This problem resembles Felsenstein's worst-case scenario (??), where a singular event on a lineage separating two clades generates a spurious association between two traits.

To investigate whether clade-level differences dominated the relationship between diversity and population size, I fit phylogenetic mixed-effects models to phyla-level subsets of the data for clades with sufficient sample sizes (see Methods: ??). This analysis shows a significant positive relationship between diversity and population size in arthropods, and positive weak relationships in molluscs and chordates (??-??). Each of the 90% credible intervals for slope overlap, suggesting the relationship between  $\pi$  and  $N_c$  is similar across these clades.

Additionally, I have explored the rate of trait change through time using node-height tests (?). Node-height tests regress the absolute values of the standardized contrasts between lineages against the branching time (since present) of these lineages. Under Brownian Motion (BM), standardized contrasts are estimates of the rate of character evolution (?); if a trait evolves under constant rate BM, this relationship should be flat. For both diversity and population size, node-height tests indicate a significant increase in the rate of evolution towards the present (robust regression p-values 0.023 and 0.00018 respectively; ??C). Considering the constituents of the population size estimate, range and body mass, separately, the rate of evolution of range but not body mass shows a significant increase (p-value  $1.03 \times 10^{-7}$ ) towards the present.



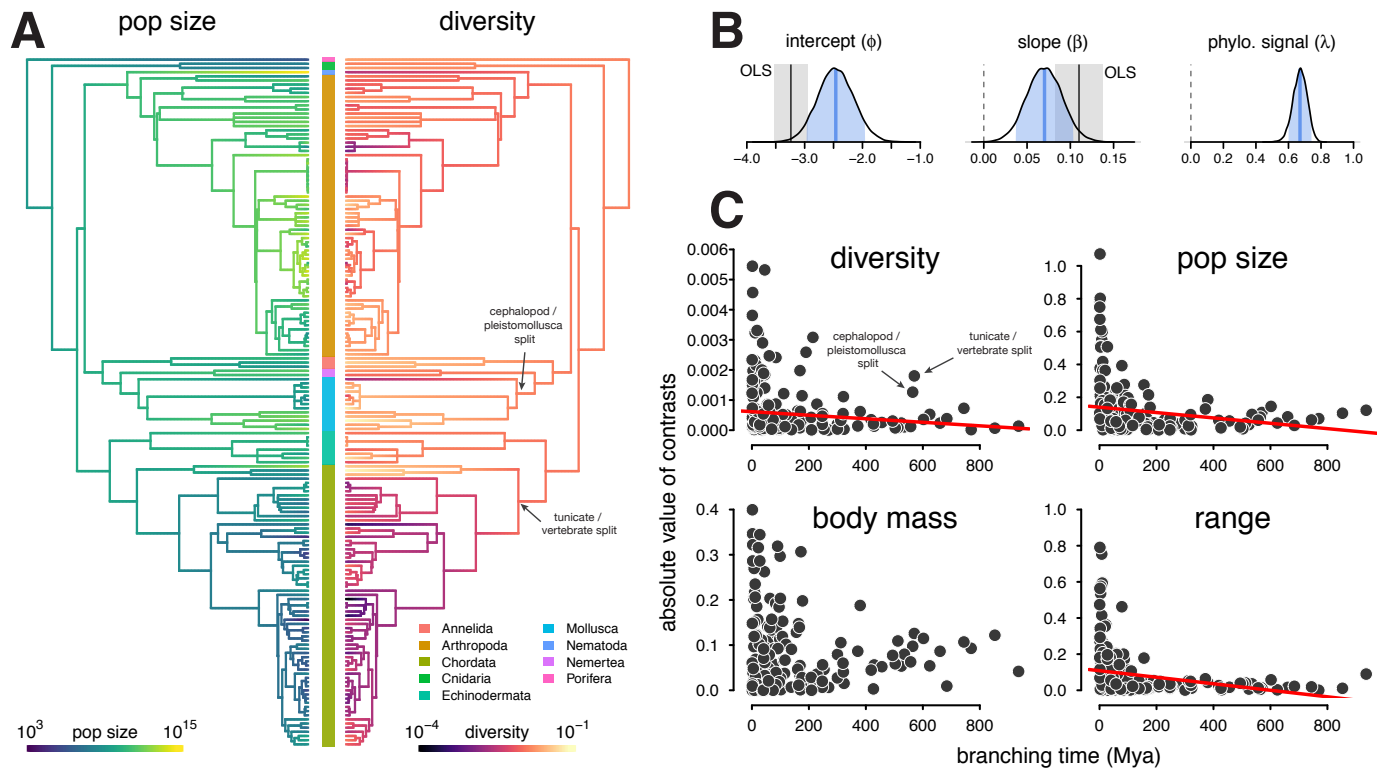


**Figure 3.** (A) The ancestral continuous trait estimates for the population size and diversity (differences per bp, log scaled) across the phylogeny of 166 taxa. The phyla of the tips are indicated by the color bar in the center. (B) The posterior distributions of the intercept, slope, and phylogenetic signal ( $\lambda$ ,  $\tau$ ) of the phylogenetic mixed-effects model of diversity and population size (log scaled). Also shown are the 90% credible interval (light blue shading), posterior mean (blue line), OLS estimate (gray solid line), and bootstrap OLS confidence intervals (light gray shading). (C) The node-height tests of diversity, population size, and the two components of the population size estimates, body mass, and range (all traits on log scale before contrast was calculated). Each point shows the standardized phylogenetic independent contrast and branching time for a pair of lineages. Red lines are robust regression estimates (and are only shown for statistically significant relationships at the  $\alpha = 0.05$  level). Note that some outlier pairs with very high phylogenetic independent contrasts were excluded (in all cases, these outliers were in the genus *Drosophila*).

**Figure 3-Figure supplement 1.** The posterior distributions for the parameters of the phylogenetic mixed-effects model of diversity and population size (this is analogous to Figure ??B) fit separately on chordates ( $n = 68$ ), molluscs ( $n = 13$ ), and arthropods ( $n = 68$ ). The phylogenetic mixed-effects model for chordates indicated the best-fitting model had no residual variance ( $\sigma_r^2 = 0$ ), so an alternate model without this variance component was used to ensure proper convergence; this model is shown in green. The light blue (green) shaded regions are the 90% credible intervals, the blue (green) lines the posterior averages, the gray shaded regions the OLS bootstrap 95% confidence intervals, and the gray lines the OLS estimate. Note that unlike ??, the OLS estimate uses all taxa, not just those present in the phylogeny, since splitting the data by phyla reduces sample sizes (OLS with just the subset of taxa in the phylogeny is not significant for either chordates and arthropods). The vertical dashed gray line indicates zero.

**Figure 3-Figure supplement 2.** The ancestral continuous trait estimates for diversity and population size with species labels.

**Figure 3-Figure supplement 3.** The ancestral continuous trait estimates for recombination map length and diversity and population size with species labels.



233 Interestingly, the diversity node-height test reveals two rate shifts at deeper splits (??C, top  
 234 left) around 570 Mya. These nodes represent the branches between tunicates and vertebrates in  
 235 chordates, and cephalopods and pleistomollusca (bivalves and gastropods) in molluscs. While the  
 236 cephalopod-pleistomollusca split outlier may be an artifact of having a single cephalopod (*Sepia*  
 237 *officinalis*) in the phylogeny, the tunicate-vertebrate split outlier is driven by the low diversity of  
 238 vertebrates and the previously-documented exceptionally high diversity of tunicates (sea squirts;  
 239 ??). This deep node representing a rate shift in diversity could reflect a change in either effective  
 240 population size or mutation rate, and there is some evidence of both in this genus *Ciona* (??). Nei-  
 241 ther of these deep rate shifts in diversity is mirrored in the population size node-height test (Figure  
 242 ??C, top right). Rather, it appears a trait impacting diversity but not census size (e.g. mutation rate  
 243 or offspring distributions) has experienced a shift on the lineage separating tunicates and verte-  
 244 brates. At nearly 600 Mya, these deep nodes illustrate that expected effective population sizes  
 245 (and thus coalescent times) can share phylogenetic history, due to phylogenetic inertia in some  
 246 combination of population size, reproductive system, and mutation rates.

247 Finally, an important caveat is the increase in rate towards the tips could be caused by measure-  
 248 ment noise, or possibly that uncertainty or bias in the divergence time estimates deep in the tree.  
 249 Inspecting the lineage pairs that lead to this increase in rate towards the tips indicates these rep-  
 250 resent plausible rate shifts, e.g. between cosmopolitan and endemic sister species like *Drosophila*  
 251 *simulans* and *Drosophila sechellia*; however, ruling out measurement noise entirely as an explana-  
 252 tion would involve considering the uncertainty of diversity and population size estimates.

## 253 Assessing the Impact of Linked Selection on Diversity Across Taxa

254 The above analyses reemphasize the drastic shortfall of diversity levels as compared to census  
 255 sizes. Linked selection has been proposed as the mechanism that acts to reduce diversity levels  
 256 from what we would expect given census sizes (???). Here, I test this hypothesis by estimating the  
 257 scale of diversity reductions expected under background selection and recurrent hitchhiking, and  
 258 comparing these to the observed relationship between  $\pi$  and  $N_c$ .

259 I quantify the effect of linked selection on diversity as the ratio of observed diversity ( $\pi$ ) to the  
 260 estimated diversity in the absence of linked selection ( $\pi_0$ ),  $R = \pi/\pi_0$ . Here,  $\pi_0$  would reflect only  
 261 demographic history and non-heritable variation in reproductive success. There are two difficul-  
 262 ties in evaluating whether linked selection could resolve Lewontin's Paradox. The first difficulty  
 263 is that  $\pi_0$  is unobserved. Previous work has estimated  $\pi_0$  using methods that exploit the spatial  
 264 heterogeneity in recombination and functional density across the genome to fit linked selection  
 265 models that incorporate both hitchhiking and background selection (??). The second difficulty is  
 266 understanding how  $R$  varies across taxa, since we lack estimates of critical model parameters for  
 267 most species. Still, I can address a key question: if diversity levels were determined by census sizes  
 268 ( $\pi_0 = 4N_c\mu$ ), are the combined effects of background selection and recurrent hitchhiking sufficient  
 269 to reduce diversity to observed levels? Furthermore, does the relationship between census size  
 270 and predicted diversity under linked selection across species,  $\pi_{BGS+HH} = R\pi_0$ , match the observed  
 271 relationship in ???

272 Since we lack estimates of key linked selection parameters across species, I parameterize the  
 273 hitchhiking and BGS models using estimates from *Drosophila melanogaster*, a species known to be  
 274 strongly affected by linked selection (?). Under a generalized model of hitchhiking and background  
 275 selection (??) and assuming  $N_e = N_c$ , expected diversity is

$$\pi_{BGS+HH} \approx \frac{\theta}{1/B(U,L) + 2N_c S(\gamma, L, J)} \quad (1)$$

276 where  $\theta = 4N_c\mu$ ,  $B(U, L)$  is the effect of background selection, and  $S(\gamma, L, J)$  is the rate of coales-  
 277 cence caused by sweeps (c.f. ?, equation 1, ? equation 20). Under background selection models  
 278 with recombination, the reduction is  $B(U, L) = \exp(-U/L)$  where  $U$  is the per diploid genome per gen-  
 279 eration deleterious mutation rate, and  $L$  is the recombination map length (???). This BGS model

is similar to models of effective population size under polygenic fitness variation, and can account for other modes of linked selection (???, see Appendix ??, ??). The coalescent rate due to sweeps is  $S(\gamma, L, J) = \gamma/LJ$ , where  $\gamma$  is the number of adaptive substitutions per generation, and  $J$  is the probability a lineage is trapped by sweeps as they occur across the genome (c.f.  $J_{2,2}$  in equation 15 of ?).

Parameterizing the model this way, I then set the key parameters that determine the impact of recurrent hitchhiking and background selection ( $\gamma$ ,  $J$ , and  $U$ ) to high values estimated from *Drosophila melanogaster* by ?. My estimate of the adaptive substitutions per generation ( $\gamma_{Dmel}$ ) based Elyashiv et al. implies a rate of sweeps per basepair of  $\nu_{BP,Dmel} \approx 2.34 \times 10^{-11}$ , which is close to other estimates from *D. melanogaster* (see ??-??A). The rate of deleterious mutations per diploid genome, per generation is parameterized using the estimate from Elyashiv et al.,  $U_{Dmel} = 1.6$ , which is a bit greater than previous estimates based on Bateman-Mukai approaches (???). Finally, the probability that a lineage is trapped in a sweep,  $J_{Dmel}$ , is calculated from the estimated genome-wide average coalescent rate due to sweeps from Elyashiv et al. (see ??-??B and Methods: ?? for more details on parameter estimates). Using these *Drosophila* parameters, I then explore how the predicted range of diversity levels under background selection and recurrent hitchhiking varies across species with recombination map length ( $L$ ) and census population size ( $N_c$ ).

Previous work has found that the impact of linked selection increases with  $N_c$  (?; see ??-??A), and it is often thought that this is driven by higher rates of adaptive substitutions in larger populations (?), despite equivocal evidence (?). However, there is another mechanism by which species with larger population sizes might experience a greater impact of linked selection: recombinational map length,  $L$ , is known to correlate with body mass (?) and thus varies inversely with population size. As this is a critical parameter that determines the genome-wide impact of both hitchhiking and background selection, I examine the relationship between recombination map length ( $L$ ) and census population size ( $N_c$ ) across taxa, using available estimates of map lengths across species (??). I find a significant non-linear relationship using phylogenetic mixed-effects models (??A; see Methods and Materials: ??). There is also a correlation between map length and genome size (??-??) and genome size and population size (??-??). These findings are consistent with both the hypothesis that non-adaptive processes increase genome size in small- $N_c$  species (?) which in turn could increase map lengths, as well as the hypothesis that map lengths are adaptively longer to more efficiently select against deleterious alleles (?). Overall, the negative relationship between map length and census size indicates linked selection is expected to be stronger in short map length, high- $N_c$  species.

Then, I predict the expected diversity ( $\pi_{BGS+HH}$ ) under background selection and hitchhiking, where  $N_e = N_c$ , and assuming all species had the rate of sweeps and strength of BGS as *D. melanogaster*. Since neutral mutation rates  $\mu$  are unknown and vary across species, I calculate the range of predicted  $\pi_{BGS+HH}$  estimates for  $\mu = 10^{-8}$ – $10^{-9}$  (using the four-alleles model, ?), and compare this to the observed relationship between  $\pi$  and  $N_c$  in ??B. Under these parameters, linked selection begins to appreciably depress diversity around  $N_c \approx 10^9$ , since  $S \approx 10^{-8}$ – $10^{-9}$  and linked selection dominates drift when  $S > 1/2N$ . Overall, this reveals two problems for the hypothesis that linked selection could solve Lewontin's Paradox. First, low to mid- $N_c$  species (census sizes between  $10^4$ – $10^{10}$ ) have sufficiently long map lengths that their diversity levels are only moderately reduced by linked selection, leading to a wide gap between predicted and observed diversity levels. For this not to be the case, the parameters that determine the strength of background selection and recurrent hitchhiking would need to be *higher* among these species than in *Drosophila melanogaster*. This would require that the rate of adaptive mutations or the deleterious mutation rate be orders of magnitude higher for species within this range than in *Drosophila*, which is incompatible with the rate of adaptive substitutions across species (?) and mutation rates (?). Furthermore, linked selection has been quantified in humans, which fall in this census size range, and has been found to be relatively weak (????). Second, while hitchhiking and BGS can reduce predicted diversity levels for high- $N_c$  species ( $N_c > 10^{10}$ ) to observed levels, this would imply available estimates of  $\pi_0$

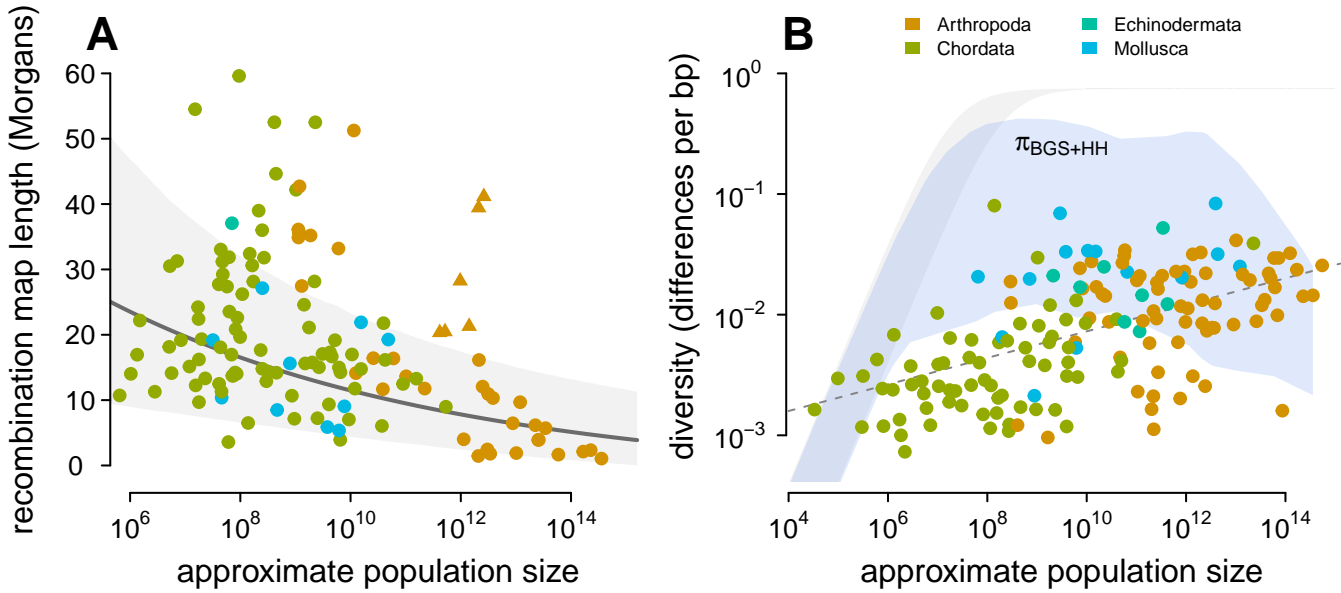


**Figure 4.** (A) The observed relationship between recombination map length ( $L$ ) and census size ( $N_c$ ) across 136 species with complete data and known phylogeny. Triangle points indicate six social taxa excluded from the model fitting since these have adaptively higher recombination map lengths (?). The dark gray line is the estimated relationship under a phylogenetic mixed-effects model, and the gray interval is the 95% posterior average. (B) Points indicate the observed  $\pi$ - $N_c$  relationship across taxa shown in ??, and the blue ribbon is the range of predicted diversity were  $N_e = N_c$  for  $\mu = 10^{-8}$ - $10^{-9}$ , and after accounting for the expected reduction in diversity due to background selection and recurrent hitchhiking under *Drosophila melanogaster* parameters. In both plots, point color indicates phylum.

**Figure 4-Figure supplement 1.** The relationship between genome size and approximate census population size. The dashed gray line indicates the OLS fit. Tiger salamander (*Ambystoma tigrinum*) was excluded because of its exceptionally large genome size ( 30Gbp).

**Figure 4-Figure supplement 2.** The relationship between genome size and recombination map length. The dashed gray line indicates the OLS fit for all taxa, and the dashed colored dashed lines indicate the linear relationship fit by phyla. Tiger salamander (*Ambystoma tigrinum*) was excluded because of its exceptionally large genome size ( 30Gbp).

**Figure 4-Figure supplement 3.** The observed  $\pi$ - $N_c$  relationship (points) across species compared to the predicted diversity (ribbons) under different modes of linked selection and parameters, for a range of mutation rates  $\mu = 10^{-8}$  --  $10^{-9}$ . In both subplots, the gray ribbon is the expected diversity if  $N_e = N_c$ . In (A), the predicted impact on diversity for four modes of linked selection are depicted: background selection (purple) and hitchhiking (yellow) individually under the parameters in the main text, and strong background selection (red) where  $U_{\text{strongBGS}} = 10U_{\text{Dmel}} \approx 16$ , and strong recurrent hitchhiking, where  $\gamma_{\text{strongHH}} = 10\gamma_{\text{Dmel}} \approx 0.23$

**Figure 4-Figure supplement 4.** The relationship between  $N_c$  and diversity in the ? data, and the relationship between estimated reduction in diversity and census size, for three different approaches.

**Figure 4-Figure supplement 5.** Comparison of the *Drosophila* sweep parameters used in this study with parameters from other studies. (A) The estimate of the number of sweeps per basepair, per genome ( $v_{\text{BP}}$ ) from Table 2 of ? (the studies included are ??? and ?); the red point is my estimate used in this paper. (B) Points are the data from ?. The blue line is the non-linear least squares fit to the data, and the green dashed line is the sweep model parameterized by the genome-wide average sweep coalescent rate  $2N.S \approx 0.92$  from the classic sweep and background selection model of ? ( $r_s$  in Supplementary Table S6).

**Figure 4-source data 1.** The map length, population size, and linked selection estimates for 136 metazoan taxa.

are underestimated by several orders of magnitude in *Drosophila* (??-??B). The high reductions in  $\pi$  predicted here (compared to those of ?) are a result of using  $N_c$ , rather than  $N_e = \pi_0/4\mu$  in the denominator of Equation (??), which leads to a very high rate of sweeps in the population. I do not consider selective interference, though the saturation of adaptive substitutions per Morgan would only act to limit the reduction in diversity (?), and thus these results are conservative. Overall, while

336 linked selection could decouple diversity from census size for high- $N_c$  species, recurrent hitchhik-  
337 ing and background selection seem unlikely to explain the observed patterns of diversity across  
338 species under our understanding of the range of parameter estimates.

## 339 Discussion

340 Nearly fifty years after Lewontin's description of the Paradox of Variation, how evolutionary, life his-  
341 tory, and ecological processes interact to constrain diversity across taxa to a narrow range remains  
342 a mystery. I revisit Lewontin's Paradox by first characterizing the relationship between genomic es-  
343 timates of pairwise diversity and approximate census population size across 172 metazoan species.  
344 Previous surveys have used allozyme-based estimates, fewer taxa, or qualitative measures of pop-  
345 ulation size. My estimates of census population sizes are quite approximate, since they use body  
346 size to predict density. An improved estimate might consider vagility (as ? did), though this is harder  
347 to do systematically across many taxa. Future work might also use other ecological information,  
348 such as total biomass, or species distribution modeling to improve census size estimates (??). Still,  
349 it seems more accurate estimates would be unlikely to change the qualitative findings here, which  
350 resemble those of early surveys (??).

351 One limitation of the dataset in this study is that diversity estimates are collated from a vari-  
352 ety of sources rather than estimated with a single bioinformatic pipeline. This leads to technical  
353 noise across diversity estimates; perhaps the relationship between  $\pi$  and  $N_c$  found here could  
354 be tighter with a standardized bioinformatic pipeline. In addition to this technical variation, there  
355 might be systematic bioinformatic sources of bias in diversity estimates. For example high-diversity  
356 sequences may fail to align to the reference genome and end up unaccounted for, leading to a  
357 downward bias. Alternatively, high-diversity sequences might map to the reference genome, but  
358 adjacent mis-matching SNPs might be mistaken for a short insertion or deletion. While these issues  
359 might adversely affect the estimates in high-diversity species, it is unlikely they will qualitatively  
360 change the observed  $\pi$ - $N_c$  relationship.

## 361 Macroevolution and Across-Taxa Population Genomics

362 Lewontin's Paradox arises from a comparison of diversity across species, yet it has been disputed  
363 whether such comparisons require phylogenetic comparative methods. Extending previous work  
364 that has accounted for phylogeny in particular clades (?), or using taxonomical-level averages (?), I  
365 show that the positive relationship between diversity and census size is significant using a mixed-  
366 effects model with a time-calibrated phylogeny. Additionally, I find a high degree of phylogenetic  
367 signal, evidence of deep shifts in the rate of evolution of genetic diversity, and that arthropods  
368 and chordates form clusters. Overall, this suggests that previous concerns about phylogenetic  
369 non-independence in comparative population genetic studies were warranted (??). Notably, Lynch  
370 (2011) has argued that PCMs for pairwise diversity are unnecessary, since mutation rate evolution  
371 is fast and thus free of phylogenetic inertia, sampling variance should exceed the variance due to  
372 phylogenetic shared history, and coalescent times are much less than divergence times. Since my  
373 findings suggest PCMs are necessary in some cases, it is worthwhile to address these points.

374 First, Lynch has correctly pointed out that while coalescent times are much less than diver-  
375 gence times and should be free of phylogenetic shared history, the factors that determine coales-  
376 cent times (e.g. mutation rates and effective population size) may not be (2011). In other words,  
377 coalescent times are free from phylogenetic shared history *were we to condition* on these causal  
378 factors that could be affected by shared phylogenetic history. My estimates of phylogenetic signal  
379 in diversity, by contrast, are not conditioned on these factors. Importantly, even "correcting for"  
380 phylogeny implicitly favors certain causal interpretations over others (??). Future work could try  
381 to untangle what causal factors determine coalescent times across species, as well as how these  
382 factors evolve across macroevolutionary timescales. Second, it is a misconception that a fast rate  
383 of trait evolution necessarily reduces phylogenetic signal (?), and that if either or both variables  
384 in a regression are free of phylogenetic signal, PCMs are unnecessary (??). The evidence of high

phylogenetic signal found in this study suggests PCMs are needed, in part to avoid spurious results from phylogenetic pseudoreplication.

Finally, beyond just accounting for phylogenetic non-independence, macroevolution and phylogenetic comparative methods are a promising way to approach across-species population genomic questions. For example, one could imagine that diversification processes could contribute to Lewontin's Paradox. If large- $N_c$  species were to have a rate of speciation that is greater than the rate at which mutation and drift reach equilibrium (which is indeed slower for large  $N_c$  species), this could act to decouple diversity from census population size. That is to say, even if the rate of random demographic bottlenecks were constant across taxa, lineage-specific diversification processes could lead certain clades to be systematically further from demographic equilibrium, and thus have lower diversity than expected for their census population size.

### **Spatial and Demographic Processes**

One limitation of this study is the inability to quantify the impact of spatial population genetic processes on the relationship between diversity and census population sizes across taxa. The genomic diversity estimates collated in this study unfortunately lack details about the sampling process and spatial data, which can have a profound impact on population genomic summary statistics (?). These issues could systematically bias species-wide diversity estimates; for example, if diversity estimates from a cosmopolitan species were primarily from a single subpopulation, diversity would be an underestimate relative to the entire population. However, biased spatial sampling alone seems incapable of explaining the  $\pi$ - $N_c$  divergence in high- $N_c$  taxa. In the extreme scenario in which only one subpopulation was sampled,  $F_{ST}$  would need to be close to one for population subdivision alone to sufficiently reduce the total population heterozygosity to explain the orders-of-magnitude shortfall between predicted and observed diversity levels. This is because the equation for  $F_{ST}$  can be rearranged such that  $H_S = (1 - F_{ST})H_T$ , where  $H_S$  and  $H_T$  are the subpopulation and total population heterozygosities; if  $H_T = 4N_c\mu$ , then only  $F_{ST} \approx 1$  can reduce  $H_S$  several orders of magnitude. Yet, across-taxa surveys indicate that  $F_{ST}$  is almost never this high within species (?). Still, future work could quantify the extent to which spatial processes contribute to Lewontin's Paradox. For example, high- $N_c$  taxa usually experience range expansions, likely with repeated founder effects and local extinction/recolonization dynamics that doubtlessly depress diversity. In particular, with the appropriate data, one could estimate the empirical relationship between dispersal distance, range size, and coalescent effective population size across taxa.

In this study, I have focused entirely on assessing the role of linked selection, rather than demography, in reducing diversity across taxa. In contrast to demographic models, models of linked selection have comparatively fewer parameters and more readily permit rough estimates of diversity reductions across taxa. Still, a full resolution of Lewontin's Paradox would require understanding how the demographic processes across taxa with incredibly heterogeneous ecologies and life histories transform  $N_c$  into  $N_e$ . With population genomic data becoming available for more species, this could involve systematically inferring the demographic histories of tens of species and looking for correlations in the frequency and size of bottlenecks with  $N_c$  across species.

### **How could selection still explain Lewontin's Paradox?**

In this study, my goal was not to accurately estimate the levels in diversity across species, but rather to give linked selection the best possible chance to solve Lewontin's Paradox. Still, I find that even after parameterizing hitchhiking and background selection with strong selection parameter estimates from *Drosophila melanogaster*, the predicted patterns of diversity under linked selection poorly fit observed patterns of diversity across species. This result extends the analysis by ? showing that levels of  $\pi_0$  estimated by ? are not decoupled from genome-wide average  $\pi$ , as would occur if linked selection were to explain Lewontin's Paradox. Here, my analysis goes a step further and suggests that models of recurrent hitchhiking and background selection are not capable of explaining the observed relationship between  $\pi$  and census size, in part because mid- $N_c$  species



434 have sufficiently long recombination map lengths to diminish the effects of even strong selection.  
435 This finding supports the idea the levels of diversity across species are primarily determined by  
436 past demographic fluctuations. Overall, while this suggests these two common modes of linked  
437 selection seem unlikely to explain across-taxa patterns of diversity, there are three major potential  
438 limitations of my approach that need further evaluation.

439 First, I approximate the reduction in diversity using homogeneous background selection and re-  
440 current hitchhiking models (??), when in reality, there is genome-wide heterogeneity in functional  
441 density, recombination rates, and the adaptive substitutions across species. Each of these factors  
442 mediate how strongly linked selection impacts diversity across the genome. Despite these model  
443 simplifications, the predicted reduction in diversity in *Drosophila melanogaster* is 85% (when using  
444  $N_e$ , not  $N_c$ ), which is reasonably close to the estimated 77% from the more realistic model of Elyashiv  
445 et al. that accounts for the actual position of substitutions, annotation features, and recombination  
446 rate heterogeneity (though it should be noted that these both use the same parameter estimates).  
447 Furthermore, even though my model fails to capture the heterogeneity of functionality density and  
448 recombination rate in real genomes, it is still extraordinary conservative, likely overestimating the  
449 effects of linked selection to see if it could be capable of decoupling diversity from census size and  
450 explain Lewontin's Paradox. This is in part because the strong selection parameter estimates from  
451 *Drosophila melanogaster* used, but also because I assume that the effective population size is equal  
452 to the census size. Even then, this decoupling only occurs in very high-census-size species, and im-  
453 plies that the diversity in the absence of linked selection,  $\pi_0$ , is currently underestimated by several  
454 orders of magnitude. Moreover, the study of ? did consider recombination rate and functional  
455 density heterogeneity in estimating the reduction due to linked selection across species, yet their  
456 predicted reductions are orders of magnitude weaker than those considered here by assuming  
457 that  $N_e = N_c$  (??-??B). Overall, even with more realistic models of linked selection, current models  
458 of linked selection seem fundamentally unable to fit the diversity-census-size relationship.

459 Second, my model here only considers hard sweeps, and ignores the contribution of soft sweeps  
460 (e.g. from standing variation or recurrent mutations; ??), partial sweeps (e.g. those that do not reach  
461 fixation), and the interaction of sweeps and spatial processes. While future work exploring these  
462 alternative types of sweeps is needed, the predicted reductions in diversity found here under the  
463 simplified sweep model are likely relatively robust to these other modes of sweeps for a few rea-  
464 sons. First, the shape of the diversity-recombination curve is equivalent under models of partial  
465 sweeps and hard sweeps, though these imply different rates of sweeps (?). Second, in the limit  
466 where most fitness variation is due to weak soft sweeps from standing variation scattered across  
467 the genome (i.e. due to polygenic fitness variation), levels of diversity are well approximated by  
468 quantitative genetic linked selection models (???). The reduction in diversity under these models  
469 is nearly identical to that under background selection models, in part because deleterious alleles  
470 at mutation-selection balance constitute a considerable component of fitness variation (see Ap-  
471 pendix Section ??; ??). Third, the parameters from ? are robust to many types of sweeps that  
472 result in substitution (e.g. see p. 19 of their Supplementary Online Materials). Finally, I also disre-  
473 garded the interaction of sweeps and spatial processes. For populations spread over wide ranges,  
474 limited dispersal slows the spread of sweeps, allowing for new beneficial alleles to arise, spread,  
475 and compete against other segregating beneficial variants (?). Through limited dispersal should  
476 act to "soften sweeps" and not impact my findings for the reasons described above, future work  
477 could investigate how these processes impact diversity in ways not captured by hard sweep mod-  
478 els.

479 Third, other selective processes, such as fluctuating selection or hard selective events, could re-  
480 duce diversity in ways not captured by the background selection and hitchhiking model. Since  
481 frequency-independent fluctuating selection generally reduces diversity under most conditions  
482 (?), this could lead seasonality and other sources of temporal heterogeneity to reduce diversity  
483 in large- $N_c$  species with short generation times more than longer-lived species with smaller pop-  
484 ulation sizes. Future work could consider the impact of fluctuating selection on diversity under

485 simple models (?) if estimates of key parameters governing the rate of such fluctuations were  
486 known across taxa. Additionally, another mode of selection that could severely reduce diversity  
487 across taxa, yet remains unaccounted for in this study, is periodic hard selective events. These se-  
488 lective events could occur regularly in a species' history yet be indistinguishable from demographic  
489 bottlenecks with just population genomic data.

## 490 Measures of Effective Population Size, Timescales, and Lewontin's Paradox

491 Lewontin's Paradox describes the extent to which the effective population sizes implied by diversity,  
492  $\tilde{N}_e$ , diverge from census population sizes. However, there are a variety other effective population  
493 size estimates calculable from different data and summary statistics (???). These include estima-  
494 tors based on the site frequency spectrum, observed decay in linkage disequilibrium, or temporal  
495 estimators that use the variance in allele frequency change. These alternate estimators capture  
496 summaries of the effective population size on shorter timescales than coalescent-based estima-  
497 tors (?), and thus could be used to tease apart processes that impact the  $N_e$ - $N_c$  relationship in the  
498 more recent past.

499 Temporal  $N_e$  estimators already play an important role in understanding another summary of  
500 the  $N_e$ - $N_c$  relationship: the ratio  $N_e/N_c$ , which is an important quantity in conservation genetics (??)  
501 and in understanding evolution in highly fecund marine species. Surveys of the short-term  $N_e/N_c$   
502 relationship across taxa indicate mean  $N_e/N_c$  is on order of  $\approx 0.1$  (???), though the uncertainty in  
503 these estimates is high, and some species with sweepstakes reproduction systems like Pacific Oys-  
504 ter (*Crassostrea gigas*) can have  $N_e/N_c \approx 10^{-6}$ . Estimates of the  $N_e/N_c$  ratio are an important, yet under  
505 appreciated piece of solving Lewontin's Paradox. For example, if  $N_e$  is estimated from the allele  
506 frequency change across a single generation (i.e. ?),  $N_e/N_c$  constrains the variance in reproductive  
507 success (???). This implies that apart from species with sweepstakes reproductive systems, the  
508 variance in reproductive success each generation (whether heritable or non-heritable) is likely in-  
509 sufficient to significantly contribute to constraining  $\tilde{N}_e$  for most taxa. Still, further work is needed  
510 to characterize (1) how  $N_e/N_c$  varies with  $N_c$  across taxa (though see ?, Figure 2), and (2) the variance  
511 of  $N_e/N_c$  over longer time spans (i.e. how periodic sweepstakes reproductive events act to constrain  
512  $N_e$ ). Overall, characterizing how  $N_e/N_c$  varies across taxa and correlates with ecology and life history  
513 traits could provide clues into the mechanisms that leads propagule size and survivorship curves  
514 to be predictive of diversity levels across taxa (??).

515 Finally, short-term temporal  $N_e$  estimators may play an important role in resolving Lewontin's  
516 Paradox. These estimators, along with short-term estimates of the impact of linked selection  
517 (?), can inform us how much diversity is depressed across shorter timescales, free from the rare  
518 strong selective events or severe bottlenecks that impact pairwise diversity. It could be that in any  
519 one generation, selection contributes more to the variance of allele frequency changes than drift,  
520 yet across-taxa patterns in diversity are better explained processes acting sporadically on longer  
521 timescales, such as colonization, founder effects, and bottlenecks. Thus, the pairwise diversity may  
522 not give us the best picture of the generation to generation evolutionary processes acting in a pop-  
523 ulation to change allele frequencies. Furthermore, certain observed adaptations are inexplicable  
524 given implied long-term coalescent effective population sizes, and are only possible if short-term  
525 effective population sizes are orders of magnitude larger (??).

## 526 Conclusions

527 In *Building a Science of Population Biology* (?), Lewontin laments the difficulty of uniting population  
528 genetics and population ecology into a cohesive discipline of population biology. Lewontin's Para-  
529 dox of Variation remains a critical unsolved problem at the nexus of these two different disciplines:  
530 across species, we fail to understand the processes that connect a central parameter of popula-  
531 tion ecology, census size, to a central parameter of population genetics, effective population size.  
532 Given that selection seems to fall short in explaining Lewontin's Paradox, a full resolution will re-  
533 quire a mechanistic understanding the ecological, life history, and macroevolutionary processes



that connect  $N_c$  to  $N_e$  across taxa. While I have focused exclusively on metazoan taxa since their population densities are more readily approximated from body mass, a full resolution must also include plant species (with the added difficulties of variation in selfing rates, different dispersal strategies, pollination, etc.).

Looking at Lewontin's Paradox through an macroecological and macroevolutionary lens begets interesting questions outside of the traditional realm of population genetics. Here, I have found that diversity and  $N_c$  have a surprisingly consistent relationship without many outliers, despite the wildly disparate ecologies, life histories, and evolutionary histories of the taxa included. Furthermore, taxa with very large census sizes have surprisingly low diversity. Is this explained by macroevolutionary processes, such as different rates of speciation for large- $N_c$  taxa? Or, are the levels of diversity we observe today an artifact of our timing relative to the last glacial maximum, or the last major extinction? Did large- $N_c$  prehistoric animal populations living in other geological eras have higher levels of diversity than our present taxa? Or, does ecological competition occur on shorter timescales such that strong population size contractions transpire and depress diversity, even if a species is undisturbed by climatic shifts or mass extinctions? Overall, patterns of diversity across taxa are determined by many overlaid evolutionary and ecological processes occurring on vastly different timescales. Lewontin's Paradox of Variation may persist unresolved for some time because the explanation requires synthesis and model building at the intersection of all these disciplines.

## Methods and Materials

### Diversity and Map Length Data

The data used in this study are collated from a variety of previously published surveys. Of the 172 taxa with diversity estimates, 14 are from ?, 96 are from ?, and 62 are from ?. The Corbett-Detig et al. data is estimated from four-fold degenerate sites, the Romiguier et al. data is synonymous sites, and the Leffler et al. data is estimated predominantly from silent, intronic, and non-coding sites. All types of diversity estimates from ? were included to maximize the taxa in the study, since the variability of diversity across functional categories is much less than the diversity across taxa. Multiple diversity estimates per taxa were averaged. The total recombination map length data were from both ? (2017; 127 taxa), and ? (2015; 9 taxa). Both studies used sex-averaged recombination maps estimated with cross-based approaches; in some cases errors in the original data were found, documented, and corrected. These studies also included genome size estimates used to create ??-?? and ??-??.

### Macroecological Estimates of Population Size

A rough approximation for total population size (census size) is  $N_c = DR$ , where  $D$  is the population density in individuals per  $\text{km}^2$  and  $R$  is the range size in  $\text{km}^2$ . Since population density estimates are not available for many taxa included in this study, I used the macroecological abundance-body size relationship to predict population density from body size. Since body length measurements are more readily available than body mass, I collated body length data from various sources (see [https://github.com/vsbuffalo/paradox\\_variation/](https://github.com/vsbuffalo/paradox_variation/)); body lengths were averaged across sexes for sexually dimorphic species, and if only a range of lengths was available, the midpoint was used.

Then, I re-estimated the relationship between body mass and population density using the data in the appendix table of ?, which includes 696 taxa with body mass and population density measurements across mammals, fish, reptiles, amphibians, aquatic invertebrates, and terrestrial arthropods. Though the abundance-body size relationship can be noisy at small spatial or phylogenetic scales (Chapter 5, ?), across deeply diverged taxa such as those included in this study and ?, the relationship is linear and homoscedastic (see ??-??). Using Stan (?), I jointly estimated the relationship between body mass from body length using the ? taxa, and used this relationship to predict body mass for the taxa in this study. These body masses were then used

to predict population density simultaneously, using the ? relationship. The code of this routine (pred\_popsizes\_missing\_centered.stan) is available in the GitHub repository ([https://github.com/vsbuffalo/paradox\\_variation/](https://github.com/vsbuffalo/paradox_variation/)).

To estimate range, I first downloaded occurrence records from Global Biodiversity Information Facility (?) using the rgbif R package (??). Using the occurrence locations, I inferred whether a species was marine or terrestrial, based on whether the majority of their recorded occurrences overlapped a continent using rnaturalearth and the sf packages (??). For each taxon, I estimated its range by finding the minimum  $\alpha$ -shape containing these occurrences. The  $\alpha$  parameters were set more permissive for marine species since occurrence data for marine taxa were sparser. Then, I intersected the inferred ranges for terrestrial taxa with continental polygons, so their ranges did not overrun landmasses (and likewise with marine taxa and oceans). I inspected diagnostic plots for each taxa for quality control (all of these plots are available in paradox\_variation GitHub repository), and in some cases, I manually adjusted the  $\alpha$  parameter or manually corrected the range based on known range maps (these changes are documented in the code data/species\_ranges.r and data/species\_range\_fixes.r). The range of *C. elegans* was conservatively approximated as the area of the Western US and Western Europe based on the map in ?. *Drosophila* species ranges are from the Drosophila Speciation Patterns website, (??). To further validate these range estimates, I have compared these to the qualitative range descriptions ? (??-??) and compared my  $\alpha$ -shape method to a subset of taxa with range estimates from IUCN Red List (??; ??-??). Each census population size is then estimated as the product of range and density.

## Population Size Validation

I validated the approximate census sizes by comparing the implied biomass of these estimates to estimates of the total carbon biomass on earth by phylum (?). For species  $i$  with wet body mass  $m_i$  and census size  $N_i$ , the implied biomass is  $m_i N_i$ . For all species in a phylum  $S$ , this total sample biomass is  $b_S = \sum_{i \in S} m_i N_i$ . I then compare this wet biomass to the carbon biomasses by phylum by ?. Across animal species, the ratio of dry to wet body mass, and carbon body mass dry body mass varies little. In their study, Bar-On et al. assume wet body mass has a 70% water content, and 50% of dry body mass is carbon mass, leading to a wet body mass to carbon mass factor of  $1-0.7/0.5 = 0.15$ . I use this factor to convert the total wet biomass to carbon biomass per phylum.

phylum	total species ( $T$ )	Bar-On et al.		Present study		Present study		prop. total species ( $f = t/T$ )	factor ( $t/f/a$ )
		biomass ( $B$ )	prop. biomass	biomass ( $b$ )	prop. biomass	num. species ( $n$ )	factor overrepresented		
Arthropoda	$1.26 \times 10^6$	1.20	0.4635	$2.80 \times 10^{-4}$	0.0102	68	0.02	$5.41 \times 10^{-5}$	4.31
Chordata	$5.41 \times 10^4$	0.87	0.3357	$2.67 \times 10^{-2}$	0.9715	68	2.89	$1.26 \times 10^{-3}$	24.40
Annelida	$1.70 \times 10^4$	0.20	0.0772	$1.23 \times 10^{-5}$	0.0004	3	0.01	$1.76 \times 10^{-4}$	0.35
Mollusca	$9.54 \times 10^4$	0.20	0.0772	$4.56 \times 10^{-4}$	0.0166	13	0.21	$1.36 \times 10^{-4}$	16.70
Cnidaria	$1.60 \times 10^4$	0.10	0.0386	$3.07 \times 10^{-5}$	0.0011	2	0.03	$1.25 \times 10^{-4}$	2.45
Nematoda	$2.50 \times 10^4$	0.02	0.0077	$4.03 \times 10^{-6}$	0.0001	1	0.02	$4.00 \times 10^{-5}$	5.03

**Table 1.** How the total carbon biomass estimates by phylum from ? compare to the implied biomass estimates from this study. All biomass estimates are carbon biomass, and the proportions are of total biomass with respect to the study. The proportion of biomass in this study compared to the Bar-On et al. estimates ? indicates chordates are overrepresented and arthropods are underrepresented in the present study; the factor that each phylum is overrepresented is given in the eighth column. Total species by phylum estimates are from ?????. The ratio column is the ratio of total biomass implied by the  $N_c$  estimates of each species in a phylum to the actual biomass of that phylum.

First, I compared the relative carbon biomass in this study to the relative carbon biomass on earth per phylum. This shows that this study's sample over represents chordate biomass (by a factor of  $\sim 3$ ), and under represents in arthropod biomass (by a factor of 0.02) relative to the proportion of carbon biomass of these phyla on earth (see column eight of Table ??). Second, to check whether the carbon biomass per phylum in the sample was broadly consistent with the total on earth by phylum ( $B_S$  for phylum  $S$ ), I calculated the expected sample biomass if species were sampled randomly from the total species in a phylum, ( $B_S \times n_S / T_S$ , where  $n_S$  is the total number of species in the sample in phylum  $S$ ,  $T_S$  is the total number of species in phylum  $S$  on earth). The fraction of total

619 species on earth included in the sample in this study is depicted in ??-??.

620 Next, I look at the ratio of sample biomass per phylum,  $b_s$  to this expected biomass per phylum  
621 (Table ??). The consistency is quite close for this rough approach and the non-random sample of  
622 taxa included in this study. The carbon biomass estimates for chordates implied by the census size  
623 estimates are ~24-fold higher than expected, but is well within reasonable expectations given that  
624 the chordate sample includes many larger-bodied domesticated species (and is a biased sample  
625 in other ways). Similarly, the implied arthropod carbon biomass is quite close to what one would  
626 expect. Overall, these values indicate that the census size estimates here do not lead to implied  
627 biomasses per phylum that are outside the range of plausibility. For other population size consis-  
628 tency checks, see Appendix ??.

## 629 **Phylogenetic Comparative Methods**

630 Of the full dataset of 172 taxa with diversity and population size estimates, a synthetic calibrated  
631 phylogeny was created for 166 species that appear in phylogenies in DateLife project (??). This  
632 calibrated synthetic phylogeny was then subset for the analyses based on what species had com-  
633 plete trait data. The diversity-population size relationship assessed by a linear phylogenetic mixed-  
634 effects model implemented in Stan (?), according to the methods described in (? see stan/phylo\_mm\_regress  
635 in the GitHub repository). This same Stan model was used to estimate the same relationship be-  
636 tween arthropod, chordate, and mollusc subsets of the data, though a reduced model was used  
637 for the chordate subset due to identifiability issues leading to poor MCMC convergence (??-??).

638 The relationship between recombination map length and the logarithm of population size is  
639 non-linear and heteroscedastic, and was fit using a lognormal phylogenetic mixed-effects model  
640 on the 130 species with complete data. Since social insects have longer recombination map lengths  
641 (?), social taxa were excluded when fitting this model. All  $\hat{R}_{\text{hat}}$  (?) values were below 1.01 and the  
642 effective number of samples was over 1,000, consistent with good mixing; details about the model  
643 are available in the GitHub repository (phylo\_mm\_lognormal.stan). Continuous trait maps (??A, ??-  
644 ??, and ??-??) were created using phyttools (?). Node-height tests were implemented based on the  
645 methods in Geiger (?), and use robust regression to fit a linear relationship between phylogenetic  
646 independent contrasts and branching times.

## 647 **Predicted Reductions in Diversity**

648 The predicted reductions in diversity due to linked selection are approximated using selection  
649 and deleterious mutation parameters from *Drosophila melanogaster*, and the recombination map  
650 length estimates from ? and ?. The mathematical details of the simplified sweep model are ex-  
651 plained in the Appendix Section ???. I use estimates of the number of substitutions,  $m$ , in genic  
652 regions between *D. melanogaster* and *D. simulans* from ?. Following ?, only substitutions in UTRs  
653 and exons are included, since they found no evidence of sweeps in introns. Then, I average over an-  
654 notation classes to estimate the mean proportion of substitutions that are beneficial,  $\alpha_{\text{Dmel}} = 0.42$ ,  
655 which are consistent with the estimates of Elyashiv et al. and estimates from MacDonald-Kreitman  
656 test approaches (see ?, Table 1). Then, I use divergence time estimates between *D. melanogaster*  
657 and *D. simulans* of  $4.2 \times 10^6$  and estimate of ten generations per year (?), calculating there are  
658  $\gamma_{\text{Dmel}} = am/2T = 2.26 \times 10^{-3}$  substitutions per generation. Given the length of the *Drosophila* au-  
659 toosomes,  $G$ , this implies that the rate of beneficial substitutions per basepair, per generation is  
660  $v_{BP, \text{Dmel}} = \gamma_{\text{Dmel}}/G = 2.34 \times 10^{-11}$ . Finally, I estimate  $J_{\text{Dmel}}$  from the estimate of genome-wide aver-  
661 age rate of sweeps from Elyashiv et al. (Supplementary Table S6) and assuming *Drosophila*  $N_e =$   
662  $10^6$ . These *Drosophila melanogaster* hitchhiking parameter estimates are close to other previously-  
663 published estimates (??-??). Finally, I use  $U_{\text{Dmel}} = 1.6$ , from ?. With these parameter estimates  
664 from *D. melanogaster*, the recombination map lengths across species, and Equation (??), I estimate  
665  $\pi_{\text{BGS+HH}}$  (assuming  $N_e = N_e$ ) across all species. This leads to a range of predicted diversity ranges  
666 across species corresponding to  $\mu = 10^{-8}$ - $10^{-9}$ ; to visualize these, I take a convex hull of all diversity  
667 ranges and smooth this with R's smooth.spline function.

## 668 **Acknowledgments**

669 I would like to thank Andy Kern and Peter Ralph for helpful discussions and supporting me during  
670 this work, and Graham Coop for inspiration and helpful feedback during socially distanced nature  
671 walks at Yolo Basin. I thank Jessica Stapley for kindly providing the recombination map length  
672 data, and Yaniv Brandvain, Amy Collins, Doc Edge, Tyler Kent, Chuck Langley, Matt Osmond, Sally  
673 Otto, Molly Przeworski, Jeff Ross-Ibarra, Aaron Stern, Anastasia Teterina, Michael Turelli, Margot  
674 Wood, and my Kern-Ralph labmates for helpful discussions. Sarah Friedman, Katherine Corn, and  
675 Josef Uyeda provided very useful advice about phylogenetic comparative methods; yet I take full  
676 responsibility for any shortcomings of my analysis. Finally, I am indebted to Guy Sella, Matt Pennell,  
677 and two other anonymous reviewers for helpful feedback. I would like to also thank UO librarian  
678 Dean Walton for helping me track down some rather difficult to find older papers. This work was  
679 supported by an NIH Grant (1R01GM117241) awarded to Andrew Kern.

681 **Simplified Sweep Effects Model**

682 I use a simplified model of the effects of recurrent hitchhiking and background selection  
 683 (BGS) occurring uniformly along a genome. Expected diversity is given by

$$684 \mathbb{E}(\pi) = \frac{\theta}{\theta + 1/B + 2NS} \quad (2)$$

$$685 \approx \frac{\theta}{1/B + 2NS} \quad (3)$$

686  
 687 (cf. equation 1 ?, and equation 20 of ?). The BGS component is given by ?,

$$688 B(U, L) = N_e \exp\left(-\frac{U}{L}\right) \quad (4)$$

689 and the hitchhiking component is

$$690 S = \frac{v_{BP}}{r_{BP}} J \quad (5)$$

691 (cf. ? equation 20) where  $J$  is the probability that two lineages coalesce down to one, given  
 692 sweeps occur uniformly along the genome. Under this homogeneous sweep model,  $J$  is

$$693 J = \int_0^L q_f(r)^2 dr \quad (6)$$

694 where  $q_f(r)$  is the approximate probability that a lineage is trapped by a sweep to frequency  
 695  $f$  when it is  $r$  recombination fraction away from this sweep (cf. ? equation 15).

696 Since I use *Drosophila melanogaster* parameter estimates from ?, I now reconcile their  
 697 model's  $S$  term with the simple model above. They estimate  $S$  in *Drosophila melanogaster*  
 698 using a composite likelihood model that considers hitchhiking and background selection  
 699 simultaneously, using substitutions and stratifying by annotation. For a neutral position at  
 700 site  $x$ , the coalescent rate due to sweeps is given by Elyashiv et al.'s equation 3,

$$701 S(x) = \frac{1}{T} \sum_{i_S} \alpha(i_S) \sum_{y \in a(i_S)} \int \exp(-r(x, y)\tau(s, N)) g(s|i_S) ds \quad (7)$$

702 where  $T$  is the number of generations that substitutions accrue,  $i_S = 1, \dots, I_S$  is the anno-  
 703 tation class (e.g. exons, introns, UTRs),  $\alpha(i_S)$  is the fraction of substitutions in annotation  
 704 class  $i_S$  that are beneficial,  $a(i_S)$  is the set of all substitutions in annotation class  $i_S$ ,  $\tau(s, N)$   
 705 is the fixation time of a site with additive effect  $s$ , and  $g(s|i_S)$  is the distribution of selection  
 706 coefficients for annotation class  $i_S$ .

707 Note, that we can recover the model of ? from this expression. Suppose there is only one  
 708 annotation class, and  $\alpha$  fraction of substitutions are beneficial, and one selection coefficient  
 709  $\bar{s}$ , (i.e.  $g(s) = \delta_0(s - \bar{s})$ ), then

$$710 S(x) = \frac{\alpha}{T} \sum_{y \in a} \exp(-r(x, y)\tau(\bar{s}, N)). \quad (8)$$

711 Let the number of substitutions be  $m := |a|$ , and imagine their positions are uniformly  
 712 distributed on a segment of length  $G$  basepairs with the focal site in the middle at position

727

728

729

730

731

$x = 0$ . Then, each substitution  $y$  is a random distance  $l_y \sim U(-G/2, G/2)$  away from the focal site. Assuming the recombination rate is a constant  $r_{BP}$  per basepair, and approximating the sum with an integral, we have,

$$S = \frac{\alpha}{T} \sum_{i=1}^m \mathbb{E}_{l_i} (\exp(-r_{BP} l_i \tau(\bar{s}, N))) \quad (9)$$

732

$$= \frac{\alpha}{TG} \sum_{i=1}^m \int_0^G \exp(-r_{BP} \ell \tau(\bar{s}, N)) d\ell \quad (10)$$

733

734

$$= \frac{\alpha m}{TG} \int_0^G \exp(-r_{BP} \ell \tau(\bar{s}, N)) d\ell \quad (11)$$

735

736

737

Using  $u$ -substitution with  $r = \ell r_{BP}$  this simplifies to

738

739

$$S = \frac{\alpha m}{TGr_{BP}} \int_0^L \exp(-r\tau(\bar{s}, N)) dr \quad (12)$$

740

741

where  $L = Gr_{BP}$ .

742

To simplify this notation, note that the rate of adaptive substitutions per basepair per generation is  $v_{BP} = \alpha m / GT$ , so

743

744

745

$$S = \frac{v_{BP}}{r_{BP}} \int_0^L \exp(-r\tau(\bar{s}, N)) dr \quad (13)$$

746

747

748

This is analogous to the second term of ? equation 17, with  $k = i = 2$  and  $x = 1$  (e.g. conditioning on a sweep to fixation). Note that there appears to be a factor of two error in ? compared to ?; here I include the factor of two. Then,

750

751

752

753

754

$$S = \frac{v_{BP}}{r_{BP}} \underbrace{\int_0^L \exp(-2r\tau(\bar{s}, N)) dr}_J \quad (14)$$

755

756

757

758

759

760

761

762

763

764

765

766

767

768

769

770

771

772

where the integral is equal to  $J$  (c.f.  $J_{2,2}$  of equation 15 in ?) since a simple model of  $q_f(r) = f \exp(-2r\tau(s, N))$  and if we condition on fixation,  $f = 1$ . This expression is useful to generalize across species, since we know  $N$  and  $L$ . Additionally, we have estimates of  $\alpha$  and  $m/T$  in *Drosophila* and other species. In Elyashiv et al, they consider the number of substitutions per generation in genic regions only; it should be noted that the number of coding basepairs varies little across species. For convenience, I define  $\gamma = \alpha m / T$  as the number of adaptive substitutions per generation per entire genome, such that  $S(\gamma, L, J) = \gamma / L J$  used in the main text. Using the estimates of  $m \approx 4.5 \times 10^5$ ,  $\alpha \approx 0.42$ , and  $T \approx 8.4 \times 10^7$  from the Supplementary Material of Elyashiv et al., I arrive at  $\gamma \approx 0.00226$  adaptive substitutions per generation, per genome. For a  $\approx 100$  megabase genome, this translates to a  $v_{BP} \approx 2.34 \times 10^{-11}$ , which is close to previous estimates (Supplementary Figure ??). For  $J$ , I use an empirical estimate calculated from the genome-wide average of the rate of coalescent events due to sweeps, from Supplementary Table S6 of Elyashiv et al. ( $r_s = 2Ns \approx 0.92$ ). This implies  $J \approx 4.46 \times 10^{-4}$ . Alternatively, I have tried using the estimated distribution of selection coefficients from Elyashiv et al., but this led to a weaker estimate of  $J$ , since the adaptive substitutions considered tend to cluster around genic regions. Note that these *Drosophila* sweep parameters I have used are close to previous estimates (Supplementary Figures ?? A and B).

## Background Selection and Polygenic Fitness Models

Throughout the main text, I use recurrent hitchhiking and background selection models to estimate the reduction in diversity due to linked selection. Another class of linked selection models, which I refer to as quantitative genetic linked selection models (QGLS; ??), can also depress genome-wide diversity. Furthermore, these models may depress diversity at neutral sites unlinked to the regions containing fitness variation. While I did not explicitly incorporate these models into my estimates of the diversity reductions, their effect is implicit in background selection models because they are analytically nearly identical. Here, I briefly sketch out the connection between BGS and QGLS models.

Under the ? model, the effective population size is  $N_e^{SC98} = N \exp(-C^2/(1-Z)L)$ , where  $C^2$  is the standardized heritable fitness variation,  $1 - Z$  is the decay of genetic variance through time, and  $L$  is the recombination map length. This model can accommodate a variety of modes of selection such as selection on an infinitesimal trait (?, p. 1016), and the flux of either weakly advantageous or deleterious alleles (?, p. 2109). If the source of fitness variation is entirely the input of new deleterious mutations with heterozygous effect  $sh$  at rate  $U$  per diploid genome per generation, then under mutation-selection balance, the equilibrium relative variance in reproductive success  $C^2 = Ush$  (?, ?, p. 167), and  $Z = 1 - sh - 1/2N_e$  (?). Thus, if  $1/2N_e \ll sh \ll 1$ , then  $C^2/(1-Z) \approx U$  and  $N_e^{SC98} \approx N \exp(-U/L)$ , which is the BGS model used in the main text and is a result of many background selection models with similar assumptions (? eqn. 15; ? eqn. 9; ? eqn. 4; ? eqn. 22b). Intuitively, the similarity of these models reflects the fact that a substantial proportion of heritable fitness variation is caused by the continual flux of deleterious alleles across the genome under mutation-selection balance (??).

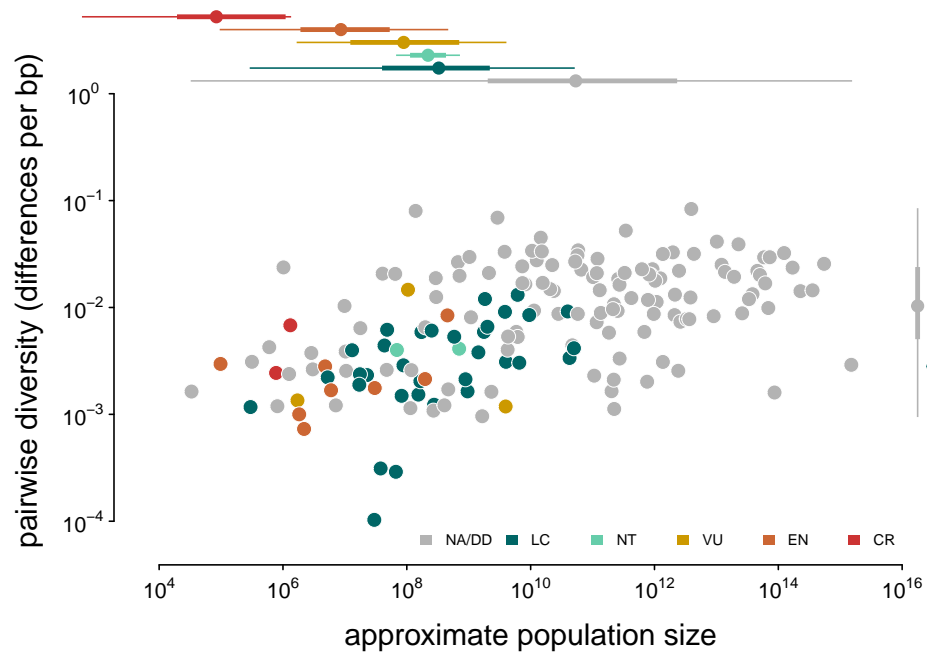


### Additional Population Size Validation

In addition to the biomass-based validation described in the main text, I also conducted a few other consistency checks. First, note that the body-mass-based estimates of density for *Drosophila* are similar to previously used estimates in surveys of census size and diversity. ? suggested a maximum of 5 *Drosophila* per m<sup>2</sup>, including regions of the range that are not inhabitable. Across *Drosophila*, the body mass based estimates suggest 10<sup>6.7</sup> – 10<sup>7.6</sup> individuals per km<sup>2</sup>, or 4.5 – 36.3 individuals per m<sup>2</sup>, which are consistent with this previous estimate. ?'s estimates of *Drosophila pseudoobscura*'s census size are four orders of magnitude smaller than mine, but their approach uses a speculated ratio of population sizes of different *Drosophila* species rather than range sizes (?, p. 81).

As another consistency check, I looked at the rank order of mammals by biomass. Whale species have the first and third highest biomass with 11.4 and 3.9 megatons of carbon biomass (for *Balaenoptera bonaerensis* and *Eschrichtius robustus*, respectively). While this seems high, a recent study shows that across whale species, pre-whaling carbon biomass was at the tens of megatons level (?, Table 1 and Figure 1). Given that my census size estimates represent populations at a macroecological equilibrium, they would not reflect reduced density due to whaling or other anthropogenic causes. Humans had the second largest biomass, followed by wolf species (*Canis lupus* and *C. latrans*); as with whales, the population sizes for wolf species represent pre-anthropogenic densities and are overestimates compared to current population sizes, as expected.

Finally, there are other estimates of approximate population sizes for some species that I compared my estimates to. The United Nation's FAOSTAT database estimates the total number of horses (*Equus caballus*) on earth as ~60 million; the estimate in this study is close to 40 million. For other domesticated species like chicken (*Gallus gallus*), estimates range from 25 million to 19.6 billion (??); the present study's estimate lies in the middle at ~175 million. Again, this is a known limitation of this method, as the range is estimated from occurrence data and does not consider species' niches. This present study's estimate of the number of king penguins (*Aptenodytes patagonicus*) is about 3 million; the population size was recently estimated as 2.23 million pairs (?).



**Appendix 4 Figure 1.** A version of ?? with points colored by their IUCN Red List conservation status. Margin boxplots show the diversity and population size ranges (thin lines) and interquartile ranges (thick lines) for each category. NA/DD indicates no IUCN Red List entry, or Red List status Data Deficient; LC is Least Concern, NT is Near Threatened, VU is Vulnerable, EN is Endangered, and CR is Critically Endangered.

## 827 Appendix 4

### 828 Diversity and IUCN Red List Status

829 I also investigated the relationship between species' IUCN Red List categories (an ordinal  
 830 scale of how threatened a species is) and both diversity and population size, finding that  
 831 species categorized as more threatened have both smaller population sizes and reduced  
 832 diversity, compared to non-threatened species (Supplementary Figure ??) consistent with  
 833 past work (?). A linear model of diversity regressed on population size has lower AIC when  
 834 the IUCN Red List categories are included, and the estimates of the effect of IUCN status  
 835 are all negative on diversity, though not all are significant in part because some categories  
 836 have three or fewer species (Supplementary Table ??).

	mean	2.5 %	97.5 %
$\beta_0$	-2.80	-3.20	-2.50
$\beta_{LC}$	-0.39	-0.57	-0.21
$\beta_{NT}$	-0.22	-0.83	0.39
$\beta_{VU}$	-0.34	-0.84	0.16
$\beta_{EN}$	-0.40	-0.73	-0.07
$\beta_{CR}$	-0.03	-0.65	0.59
$\beta_{N_c}$	0.08	0.05	0.11

**Appendix 4 Table 1.** The regression estimates of full IUCN Red List population size model for diversity,  $\log_{10}(\pi) = \beta_0 + \beta_{LC}LC + \beta_{NT}NT + \beta_{VU}VU + \beta_{EN}EN + \beta_{CR}CR + \beta_{N_c}\log_{10}(N_c)$ ;  $df = 165$ . Using AIC to compare this full model to a reduced model of  $\log_{10}(\pi) = \beta_0 + \beta_{N_c}\log_{10}(N_c)$ ,  $AIC_{full} = 204.9$ ,  $AIC_{reduced} = 216.4$ .

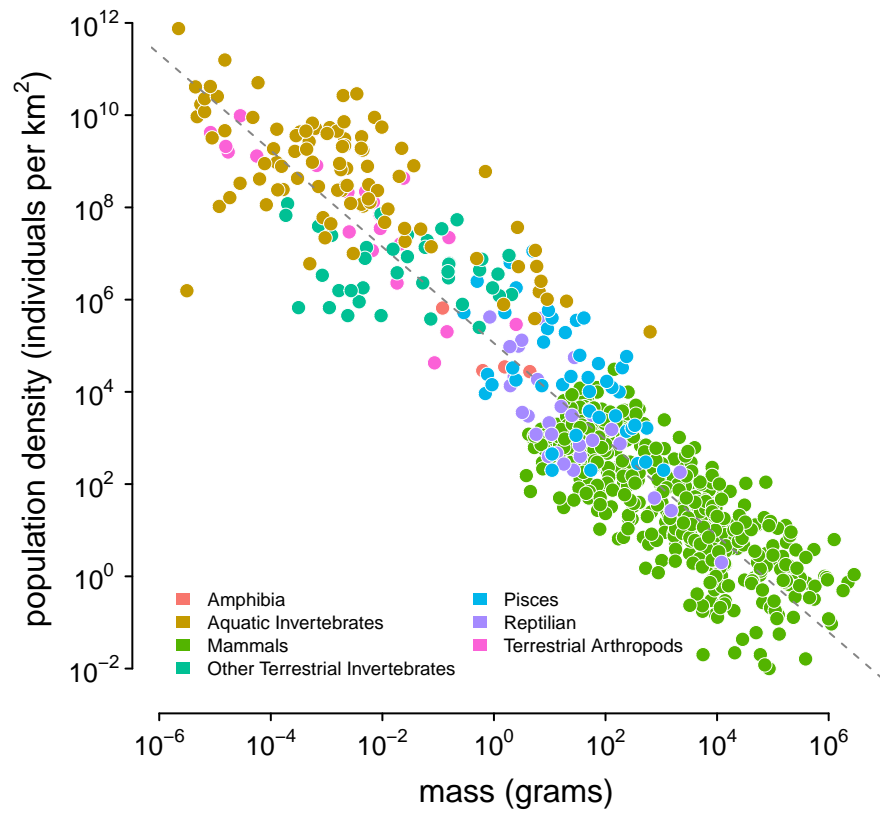


**Figure 1–Figure supplement 1.** The source of this data is appendix table of ?; the color indicates Damuth's original group labels. The dashed line was estimated using a lognormal regression model in Stan. References to each measurement are available in ?.

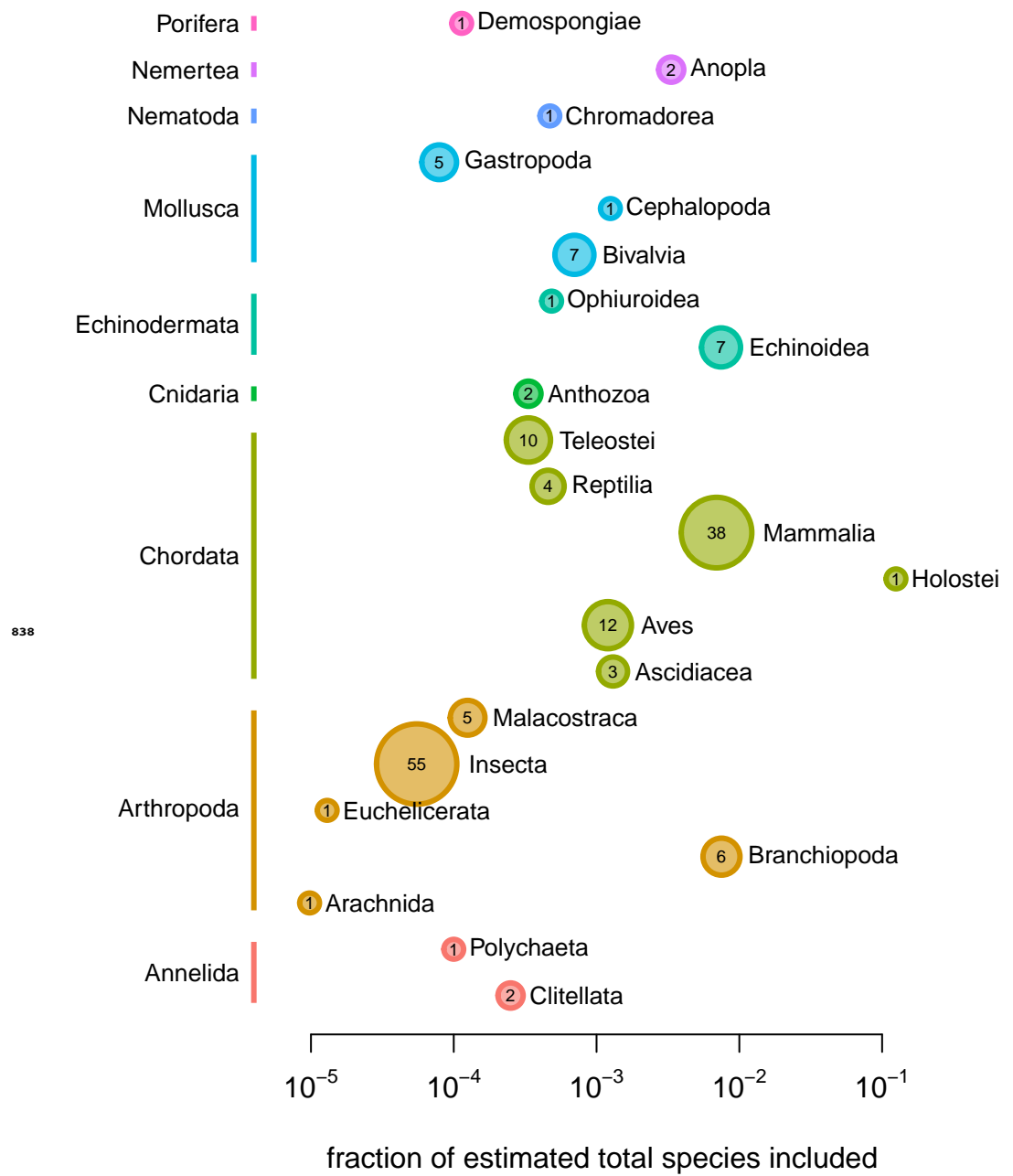


**Figure 1–Figure supplement 2.** The color of the points represents phylum, and the size of the point represents the absolute number of species by class.

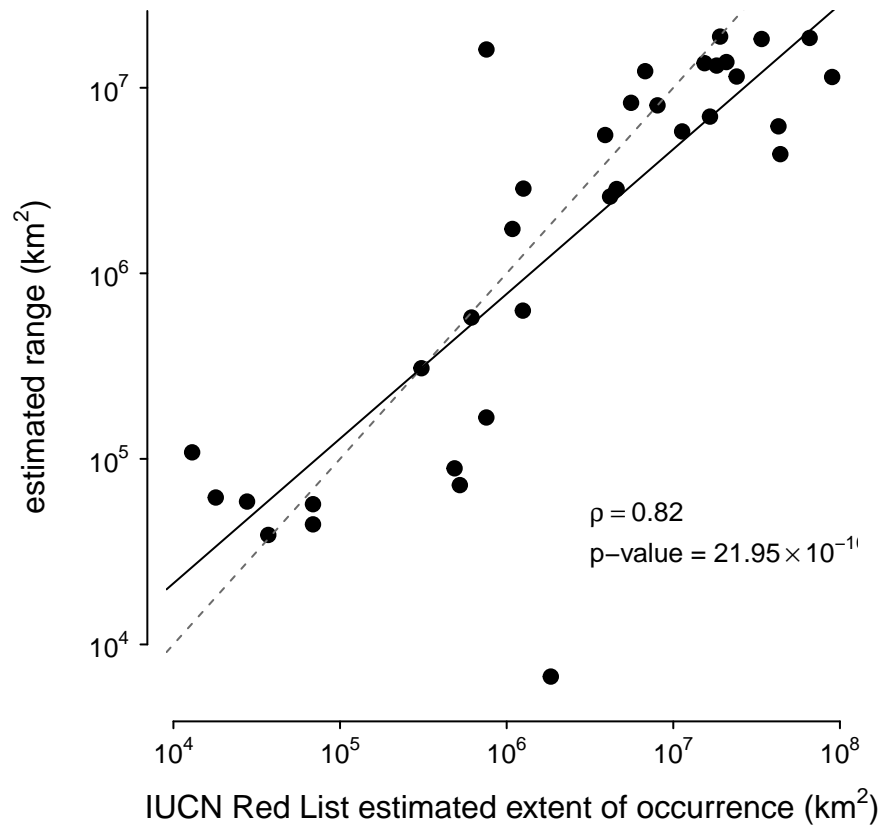


**Figure 1–Figure supplement 3.** The correspondence between the ranges estimated with the alpha hull method applied to GBIF data used in this paper and IUCN Red List’s Extent of Occurrence for the subset of species in both datasets. Note that the IUCN Red List contains predominantly endangered species, which leads to ascertainment bias; still, the high correlation between the estimated ranges shows the alpha hull method works well.

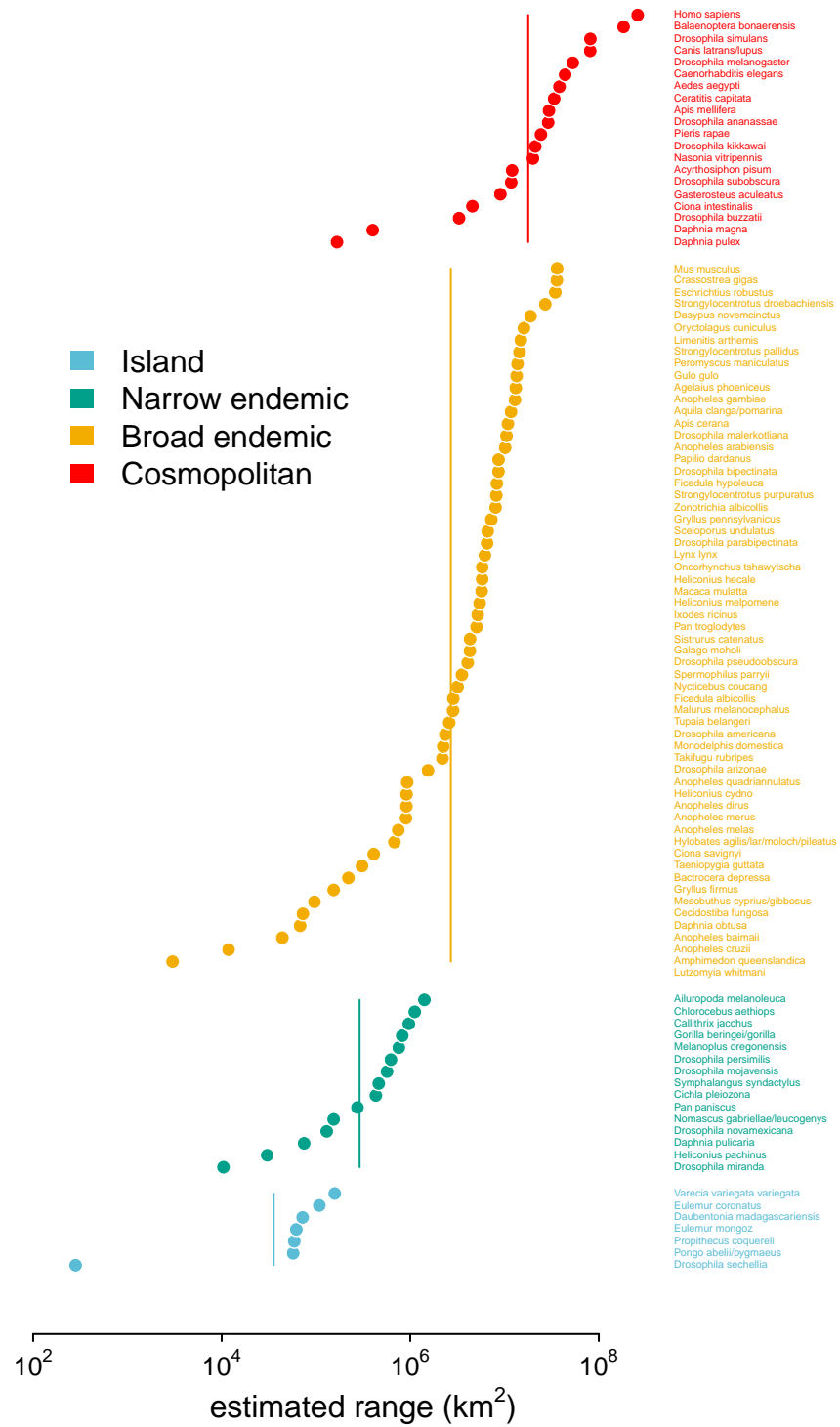


**Figure 1–Figure supplement 4.** The estimated ranges using GBIF occurrence data, ordered within and colored by the original range category labels assigned in ?.



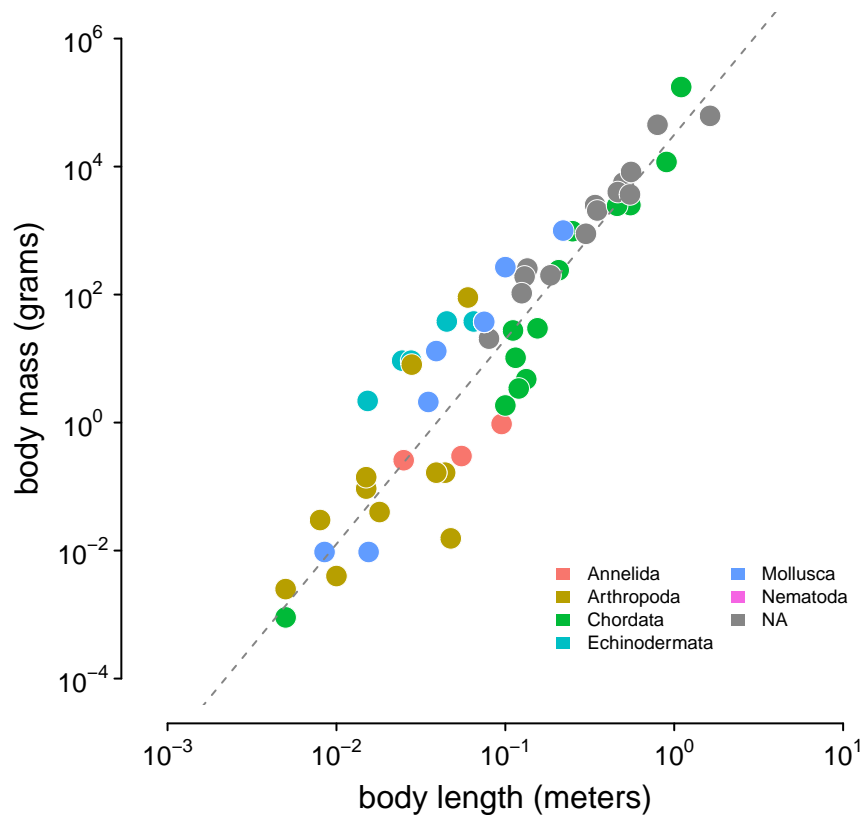


**Figure 1-Figure supplement 5.** The relationship between body length (meters) and body mass (grams) in the ? data set. This is used to infer body masses for taxa. The gray dashed line is the line of best fit inferred using Stan.

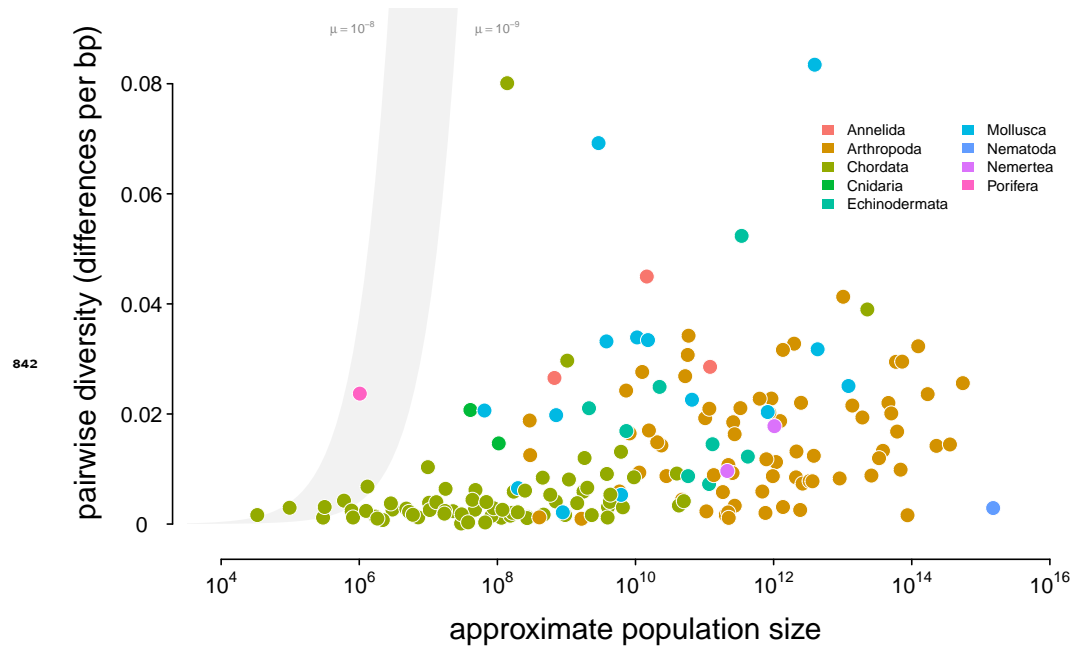


**Figure 2-Figure supplement 1.** A linear-log version of Figure 2. Points are colored by phylum, and the shaded region is the predicted neutral level of diversity assuming  $N_e = N_c$  with mutation range ranging between  $10^{-10} \leq \mu \leq 10^{-8}$ .

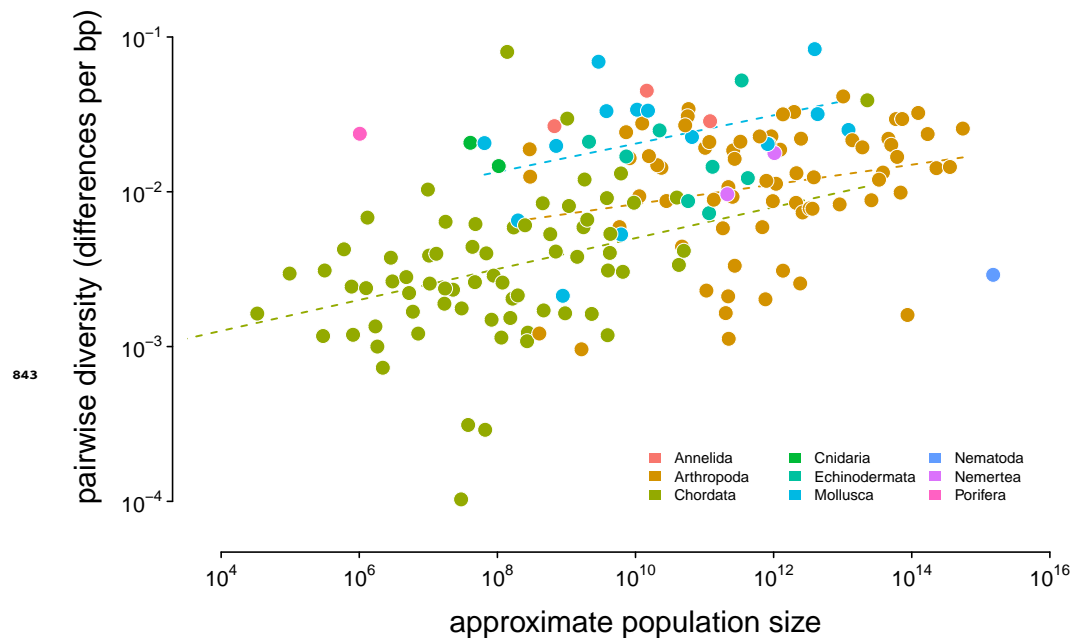


**Figure 2-Figure supplement 2.** A version of Figure 2 with OLS estimates per phylum. Diversity and approximate population size for 172 taxa, colored by phylum; the dashed lines indicate the non-phylogenetic OLS estimates of the relationship between population size and diversity grouped by phyla.

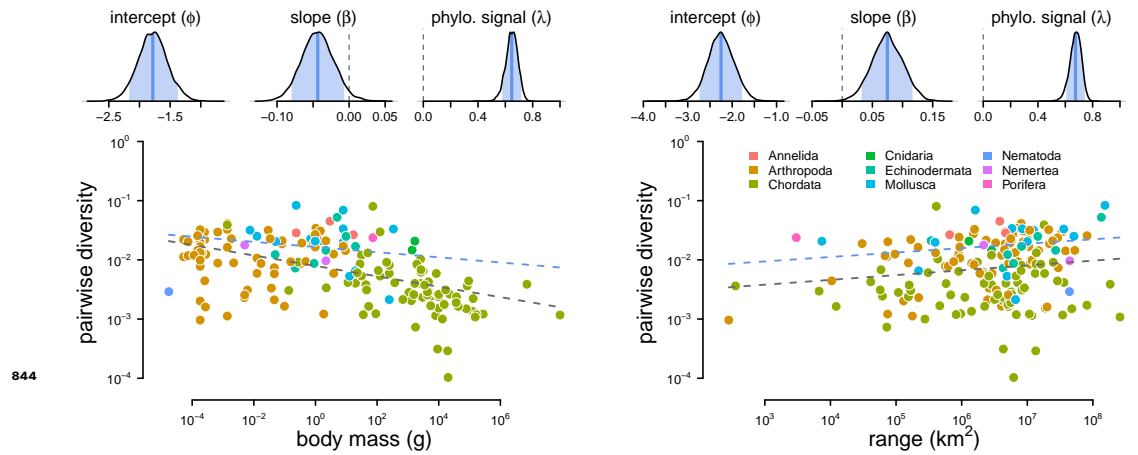


**Figure 2-Figure supplement 3.** The posterior distributions and fitted relationship between diversity and both body mass and range size. The relationship between diversity (differences per basepair) and body mass (left) and range (right) across 172 species. The top row are posterior distributions of parameters estimated using the phylogenetic mixed-effects model using 166 taxa in the synthetic phylogeny for the intercept, slope, and phylogenetic signal from the mixed-effects model. The bottom row contain each species as a point, colored by phyla. The gray dashed line is the non-phylogenetic standard regression estimate, and the blue dashed line is the relationship fit by the phylogenetic mixed-effects model.

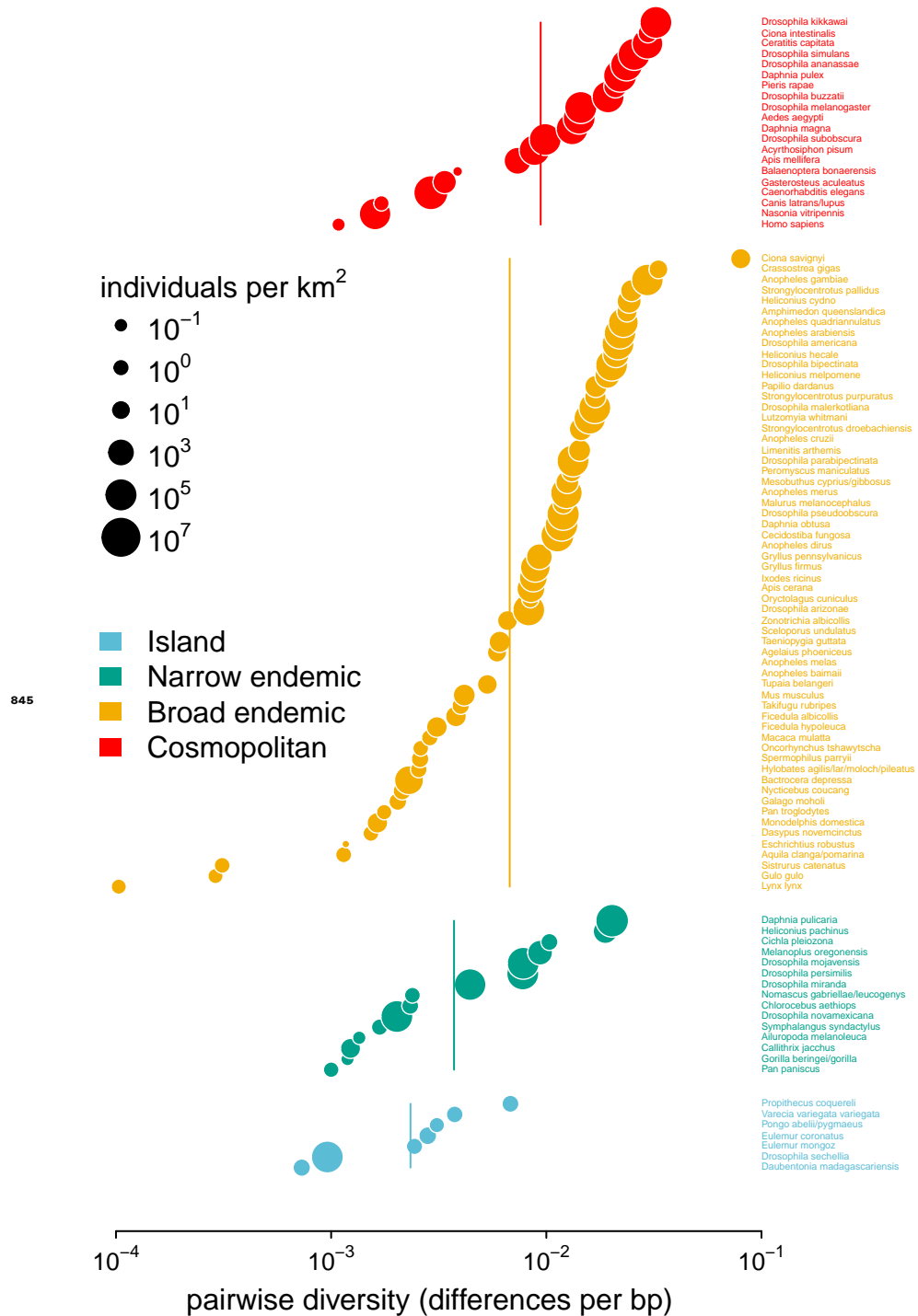


**Figure 2-Figure supplement 4.** Pairwise diversity grouped by the range categories from ?, with point size indicating the predicted population density. The vertical lines are the range category group means.

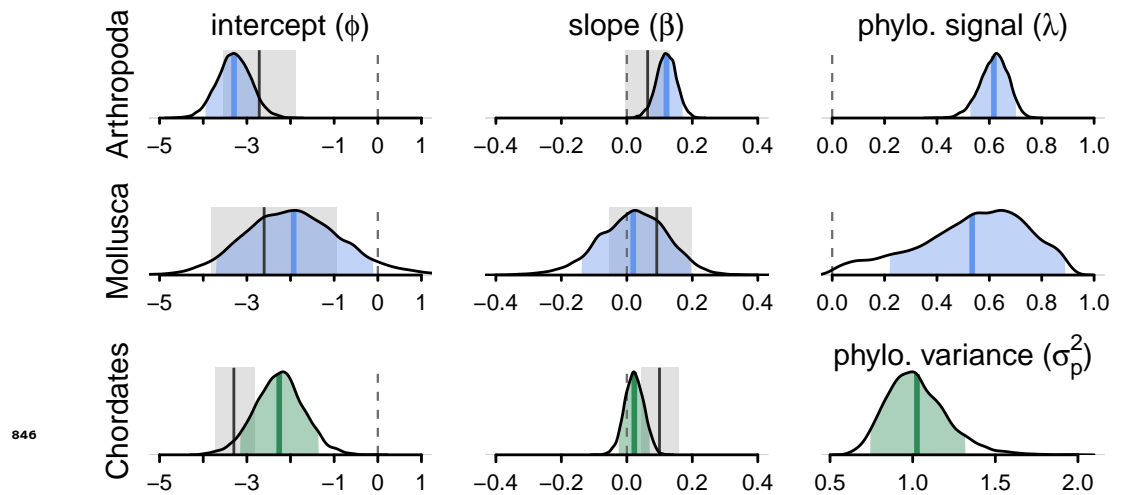


**Figure 3-Figure supplement 1.** The posterior distributions for the parameters of the phylogenetic mixed-effects model of diversity and population size (this is analogous to Figure ??B) fit separately on chordates ( $n = 68$ ), molluscs ( $n = 13$ ), and arthropods ( $n = 68$ ). The phylogenetic mixed-effects model for chordates indicated the best-fitting model had no residual variance ( $\sigma_r^2 = 0$ ), so an alternate model without this variance component was used to ensure proper convergence; this model is shown in green. The light blue (green) shaded regions are the 90% credible intervals, the blue (green) lines the posterior averages, the gray shaded regions the OLS bootstrap 95% confidence intervals, and the gray lines the OLS estimate. Note that unlike ??, the OLS estimate uses all taxa, not just those present in the phylogeny, since splitting the data by phyla reduces sample sizes (OLS with just the subset of taxa in the phylogeny is not significant for either chordates and arthropods). The vertical dashed gray line indicates zero.



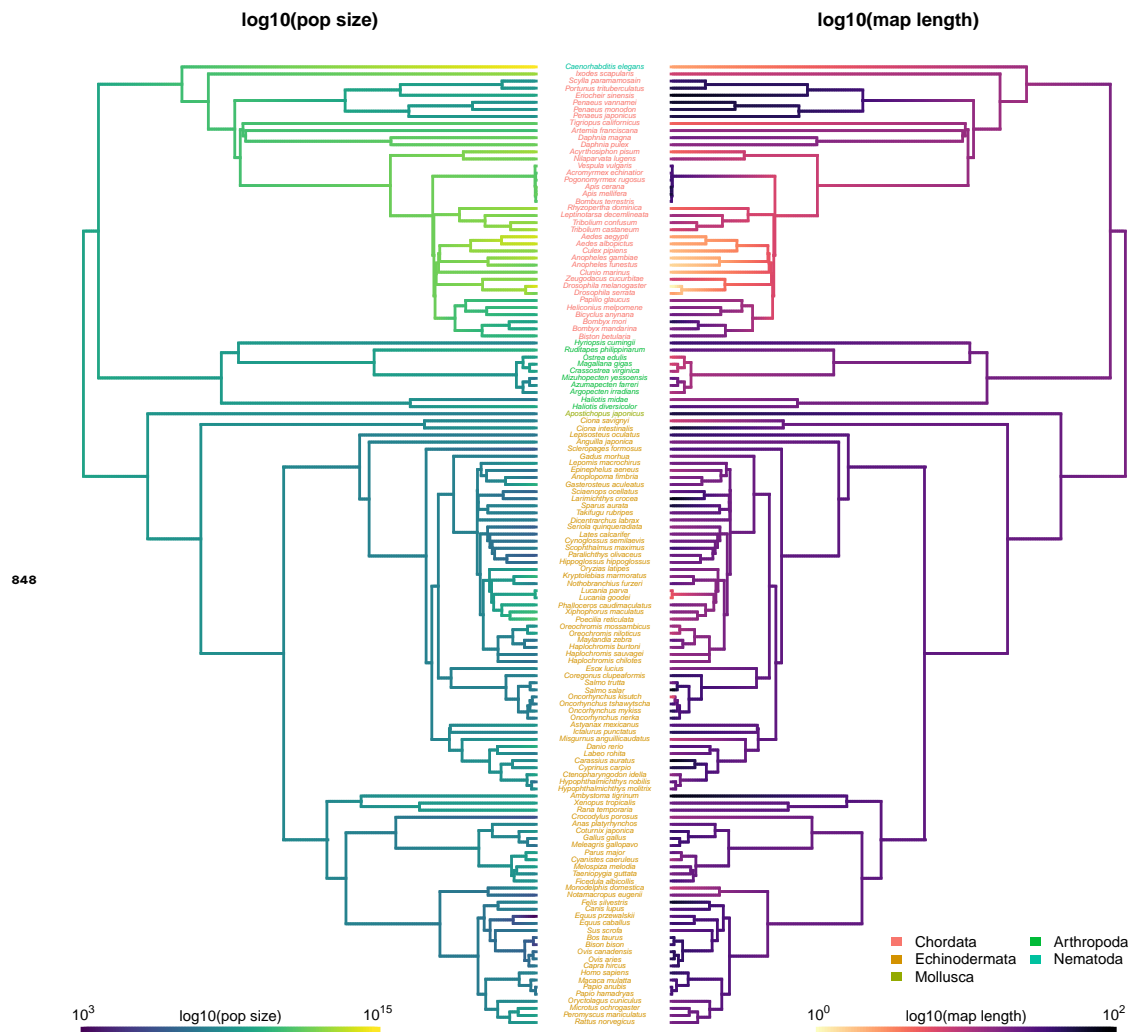


**Figure 3—Figure supplement 3.** The ancestral continuous trait estimates for recombination map length and diversity and population size with species labels.



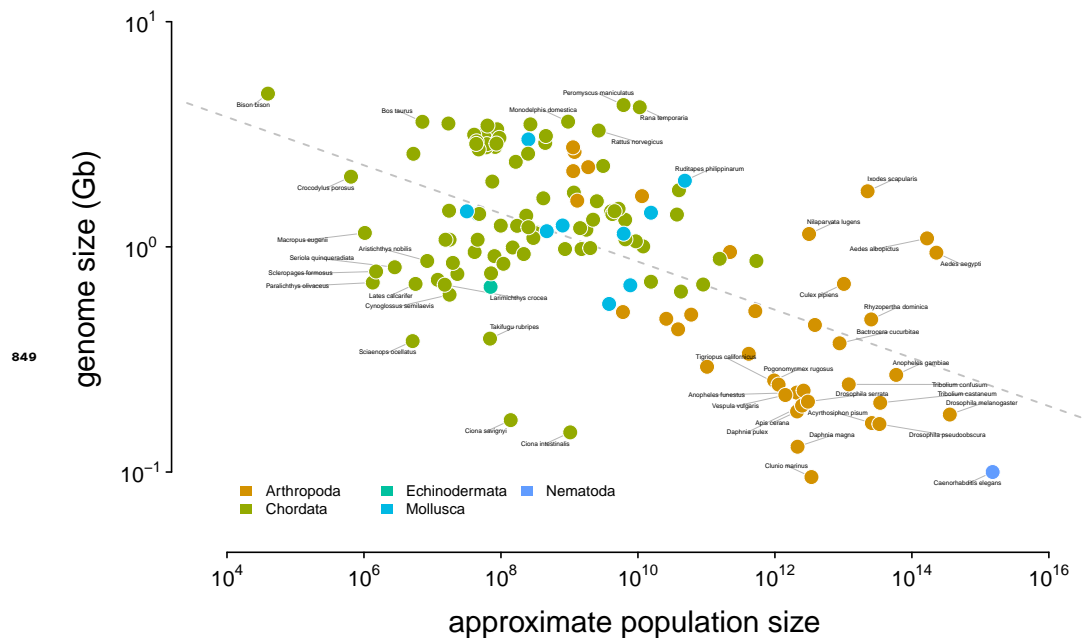


**Figure 4–Figure supplement 1.** The relationship between genome size and approximate census population size. The dashed gray line indicates the OLS fit. Tiger salamander (*Ambystoma tigrinum*) was excluded because of its exceptionally large genome size (30Gbp).

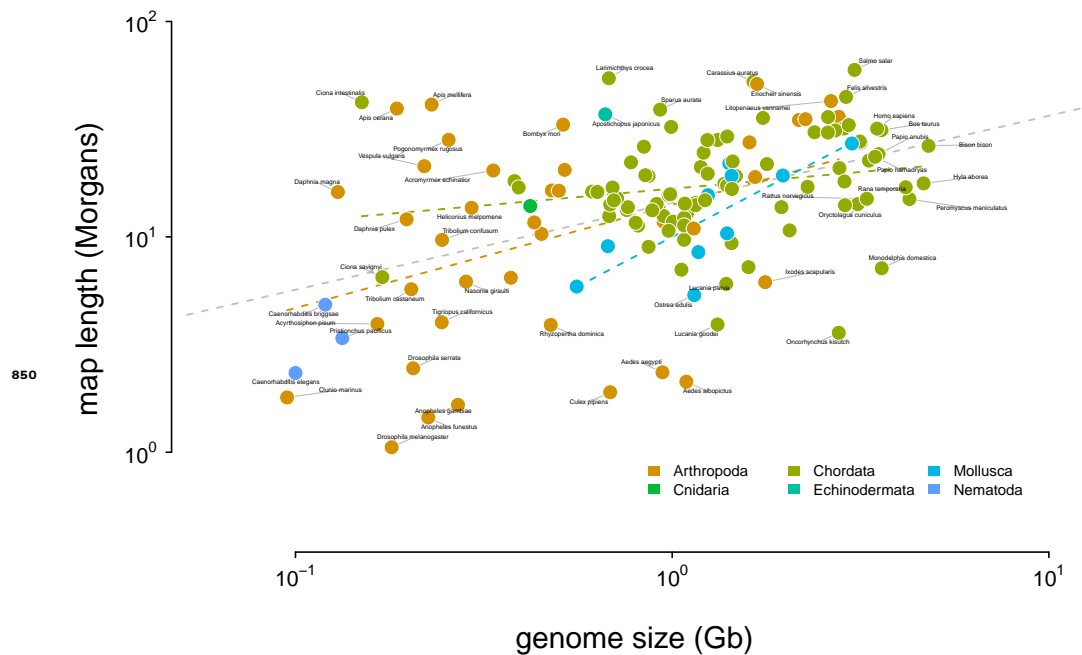


**Figure 4–Figure supplement 2.** The relationship between genome size and recombination map length. The dashed gray line indicates the OLS fit for all taxa, and the dashed colored dashed lines indicate the linear relationship fit by phyla. Tiger salamander (*Ambystoma tigrinum*) was excluded because of its exceptionally large genome size (30Gbp).

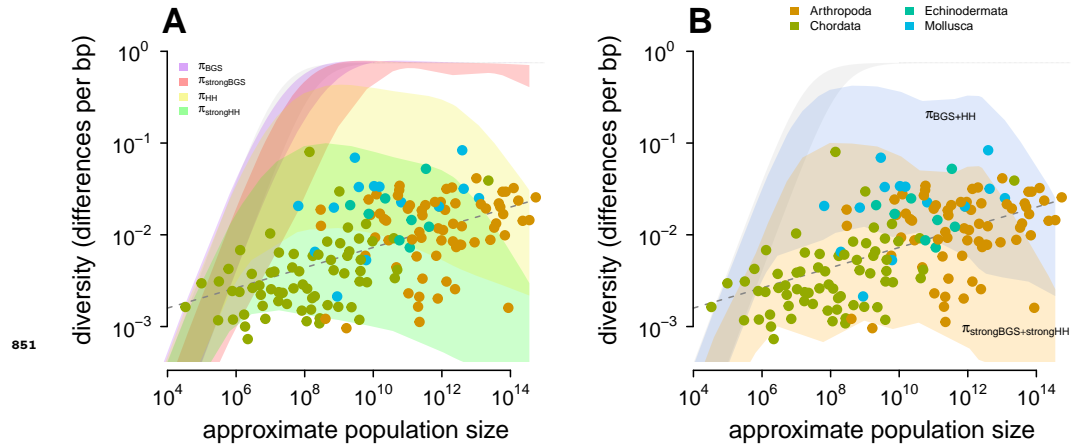


**Figure 4-Figure supplement 3.** The observed  $\pi$ - $N_e$  relationship (points) across species compared to the predicted diversity (ribbons) under different modes of linked selection and parameters, for a range of mutation rates  $\mu = 10^{-8} - 10^{-9}$ . In both subplots, the gray ribbon is the expected diversity if  $N_e = N_c$ . In (A), the predicted impact on diversity for four modes of linked selection are depicted: background selection (purple) and hitchhiking (yellow) individually under the parameters in the main text, and strong background selection (red) where  $U_{\text{strongBGS}} = 10U_{\text{Dmel}} \approx 16$ , and strong recurrent hitchhiking, where  $\gamma_{\text{strongHH}} = 10\gamma_{\text{Dmel}} \approx 0.23$

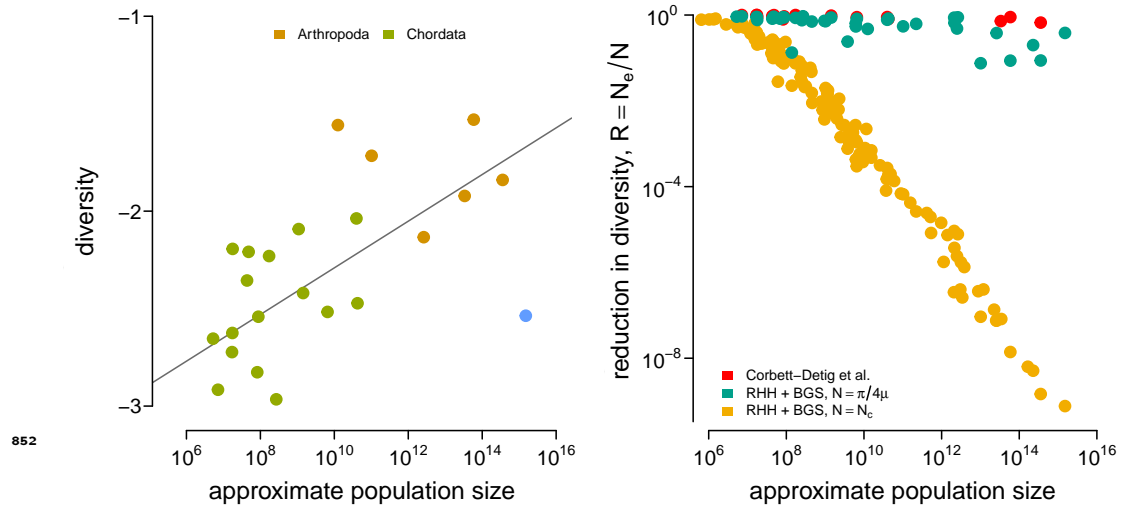


**Figure 4-Figure supplement 4.** (A) The diversity data from ? and the census population size estimated here for metazoan taxa. (B) The reductions in diversity,  $R = N_e/N$ , plotted against census size across species. The red points are the reductions estimated by ?. This confirms ?'s (2015) finding that the impact of selection ( $I = 1 - R$ ) increases with census population size (though, in the original paper size body size and range were used as separate proxy variables for census population size). The green and red points are the predicted reduction in diversity under the recurrent hitchhiking (RHH) and background selection (BGS) model using the *Drosophila melanogaster* parameters as described in the main text. The reduction in the diversity due to sweeps, from Equation 1, is determined by the term  $2N_e S$ . Green points treat  $N$  as the implied effective population size from diversity  $\tilde{N}_e = \hat{\pi}/4\mu$ , assuming  $\mu = 10^{-9}$ . Yellow points treat  $N$  as the census size,  $N = N_c$ . Overall, using the census size, e.g.  $2N_c S$ , leads to reductions in diversity that far exceed the empirical estimates of Corbett-Detig et al. and reasonable model-based predictions from  $\tilde{N}_e$ .

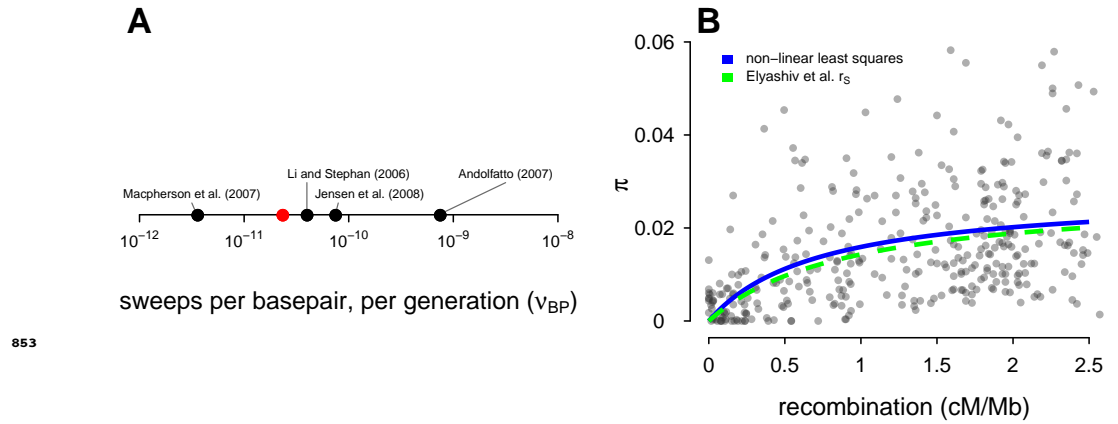


**Figure 4-Figure supplement 5.** Comparison of the *Drosophila* sweep parameters used in this study with parameters from other studies. (A) The estimate of the number of sweeps per basepair, per genome ( $v_{BP}$ ) from Table 2 of ? (the studies included are ??? and ?); the red point is my estimate used in this paper. (B) Points are the data from ?. The blue line is the non-linear least squares fit to the data, and the green dashed line is the sweep model parameterized by the genome-wide average sweep coalescent rate  $2N.S \approx 0.92$  from the classic sweep and background selection model of ? ( $r_s$  in Supplementary Table S6).